Università degli Studi di Padova

Scuola di Ingegneria

Dipartimento di Ingegneria Civile, Edile ed Ambientale

MULTISPECIES VEGETATION PATTERNS IN ARID TO SEMI-ARID LANDS

Tesi di Laurea Magistrale in Ingegneria Civile

Curriculum Idraulica

Laureanda: Chiara CALLEGARO

Relatrice: prof.ssa Nadia URSINO

A.A. 2013/2014

Table of contents

Introduction

Vegetation patterning in arid to semi-arid lands is nowadays a hot topic in eco-hydrology.

Patterned landscapes are recognized to be a fingerprint of climate and human impact on the fragile semi-arid ecosystems. They concern crucial themes as ecosystem resilience and efficient use of resources. Besides, the evident correlation between water distribution and vegetation bands dynamics offers interesting opportunities to investigate some particular hydrological phenomena in water scarcity conditions.

Many studies have been carried out on banded vegetation patterns, most of them describing the dynamics of one generic plant species in relation to the dynamic of water, but there is still a lack of focus on the fact that most of the banded patterns are composed by at least two species, and these two species are likely to occupy different sites within a band, determining a floristic zonation. This zonation is very significant because a corresponding zonation is found in soil conditions. Hydrological phenomenon is therefore strictly correlated to floristic zonation too, because infiltration, run-off/run-on, belowground water storage and evaporation-transpiration fluxes all depend on soil conditions and root activity.

We address here to multispecies dynamics in vegetation patterns in arid to semi-arid lands. The purpose of this work is to investigate whether competition-facilitation mechanisms between coexisting species may explain the pattern zonation and what the role of each species is in pattern emergence and maintenance.

1 Tiger bush: a particular self-organized vegetation pattern

Vegetation patterns are a feature of many landscapes around the world. In arid and semi-arid regions, a particular type of pattern has been observed, which is generally referred to as *tiger bush*, because it resembles the fur of a tiger when seen from above.

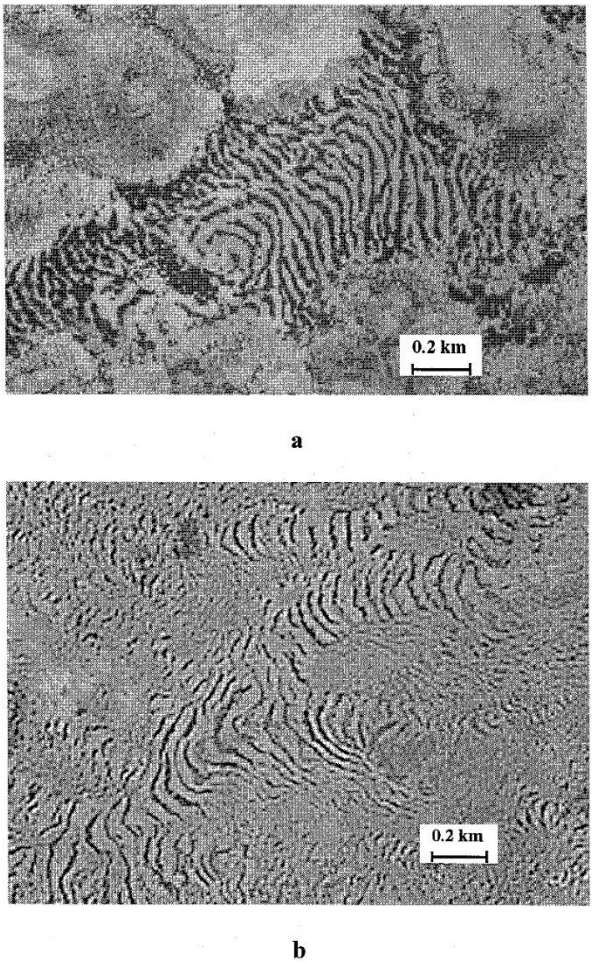

Figure 1: Typical type of banded vegetation pattern (a) in Niger (13◦400N, 2◦400E, 80 km East of Niamey, Institut Géographique National aerial photograph, AOF 1950) and (b) Somalia (9◦310N; 49◦110E, in the vicinity of Qardho, SPOT XS image of 30 May 1988, KJ 159/331). Image reproduced from *(Valentin, D'Herbès, & Poesen, Soil and water components of banded vegetation patterns, 1999)*.

Vegetation patterns were first discovered and described by Macfadyen in British Somaliland (Macfadyen, 1950), (Macfadyen, 1950) but the term tiger bush was later introduced by

Clos-Arceduc, who observed them in Niger (Clos-Arceduc, 1956). Examples of vegetation patterns are found in multiple sites all over the world, where the climate is arid to semi-arid, including Somalia, Sudan, Burkina Faso, Niger, South Africa, Jordan, Spain, Mexico, United States, Argentina, Chile, Australia, and Japan. The discovery and study of these landscapes was allowed by aerial photographs, as they are hardly detectable on the ground. A tiger bush generally looks like a bi-component mosaic, formed by vegetated stripes regularly alternating with stripes of bare soil, the width of the stripes generally going from approximately 10 meters up to hundreds of meters. Other common forms for the vegetation thickets are arcs, labyrinths or spots. The vegetation can consist of grass, shrubs or trees, or combinations of these. The phenomenon is not specific to particular species of vegetation, particular soil characteristics or particular topographic conditions, though many studies have identified an upper limit for slope, and a range for annual rainfall along with other limit conditions, and these limits are interdependent. A common explanation for the occurring of vegetation patterns is that in scarcity of resources, a quite homogeneous cover of vegetation is not a sustainable condition. Water and nutrients are intercepted by vegetation, the more vegetated areas being able to intercept a major quantity of them, while in the least vegetated areas, resources interception is not efficient, due to the low root density, so that if plant density is even slightly non uniform, local gradients in concentration of resources are determined. The most favourable conditions for plant survival is therefore found where a higher density of plants already existed (local cooperation effects), while the areas that were previously less vegetated become less and less apt to plant life (inhibition effects). This feedback mechanism causes a quite homogeneous initial density of vegetation to degenerate in a succession of highly vegetated areas and bare soil. Many authors have collected information about vegetation patterns since their discovery in the years 1950s, but a more intensive study started in the late years 1990s, when the first mathematical models were proposed to describe the genesis and characteristics of the patterns. Most models that

have been proposed explain the formation of patterns basing on deterministic mechanisms. These models may be classified as: kernel-based models, Turing instability models, or differential flow models (Borgogno, D'Odorico, Laio, & Ridolfi, 2009).

Kernel-based models, such as the one of Lefever and Lejeune (Lefever & Lejeune, O., 1997), attribute the formation and evolution of vegetation patterns to an interplay between short-range cooperative action for reproduction and long-range competition for environmental resources by plants, and mathematically model these effects by a kernel function, the sign of which is distance depending . The models based on Turing instability (Turing, 1952), (Murray, 2002), such as the one proposed by HilleRisLambers, Rietkerk et al. (HilleRisLambers, Rietkerk, van den Bosch, Prins, & de Kroon, 2001), attribute the formation of patterns to a diffusion-driven instability. In a dynamic system, the two (or more) species tend to reach a homogeneous steady state when diffusion is absent, conversely, diffusion may lead to pattern formation in response to a small linear perturbation under particular conditions, if the species have different diffusivity. Another group of models describe the dynamic system of a tiger bush not only with diffusion terms, but also with an advective term for (at least) one of the species. Between these, the model of Klausmeier (Klausmeier, 1999) is well-known and has been the base for further modelling (Ursino, 2005) (Ursino, 2007).

1.1 Main features of a tiger bush

Authors as Thiéry, Valentin and D'Herbès (Thiery, D'Herbes, & Valentin, 1995) (Valentin & D'Herbès, 1999) (Valentin, D'Herbès, & Poesen, 1999) described the typical cross-section of the tiger bushes they studied in Niger. From uphill to down-hill, five zones may be identified with regard to vegetation and crust typology (see Figure *2*): a degraded zone (D) at the bottom of the vegetated area, a bare area where run-off occurs (R), a sedimentation zone

at the top of the next vegetated zone, where water and nutrients start to be intercepted (S), a pioneer zone (P) and the core of the band (C). The two zones (P) and (C) are both vegetated, but with different plant species.

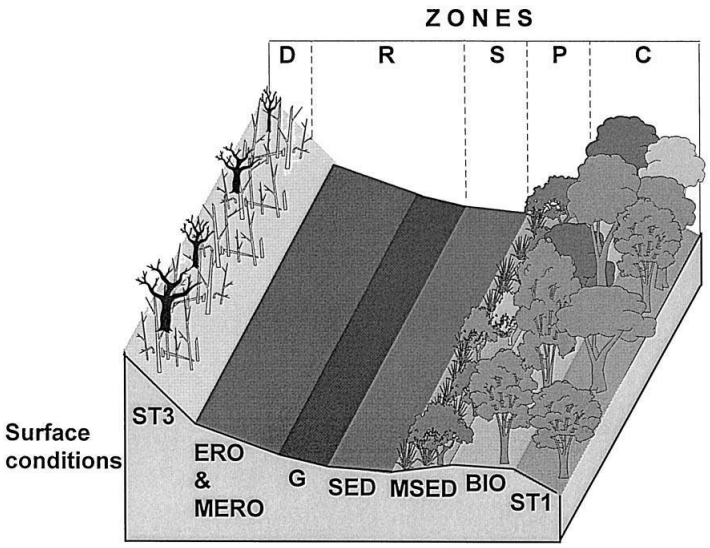

Figure 2: Schematic cross-section across a tiger bush wavelength showing the different zones. Image reproduced from *(Valentin & D'Herbès, 1999)*.

In particular, soil infiltrability and other soil properties vary in the different areas. In the degraded zone, vegetation decay due to insufficient water supply leads to the formation of structural crusts of low infiltrability. The run-off zone consists of a succession of crusts, formed by erosion (wind and water flow tend to compact very fine particles, resulting in a smooth and hard surface layer), or due to the presence of gravel, the crusts generate an intensive run-off, but the absence of incised channels proves that water flows in sheets even in this part of the section. In the sedimentation zone, at the end of the inter-band, erosion and gravel crusts are covered with sedimentary crusts, which usually crack forming curled plates during the dry periods, while during the wet periods water may pond in small depressions. The pioneer front zone is colonized by pioneer grassy vegetation which is able to penetrate in the cracks. In the central zone, the plant roots and the active termite mounds disgregate the soil crusts and increase soil porosity, and a thick litter layer protect the soil

surface from the rainfall impact. The soil properties along the cross-section are shown in Table 1.

Table 1: Main features and properties of the different surface conditions in the Nigerien tiger bush. Table reproduced from (Valentin & D'Herbès, 1999)

Type	Structure	Thickness [mm]	Infiltrability [mm ha^{-2}]	Mean run-off coefficient (Rc) [%]	Zone
Structural crusts					
Slaking (ST1)	rough surface, weak textural differentiation, weak void interconnection	1-3	5-8	35	C
Sieving (ST3)	coarse sandy layer at the top, vesicular fine sandy layer, seal of fine particles at the bottom	2-10	0-5	50	R
Coarse pavement (G)	similar to the sieving crust including coarse fragments and much pronounced vesicular porosity	2-30	0-2	90	R
Erosion crusts (ERO)	smooth exposed seal made of fine cemented particles, possible vesicles	<1	0-2	85	R
Microphytic erosion (MERO)	similar to ERO but colonised by microphytes as algae	<1	0-2	85	R
Depositional crusts					
Run-off (ROF)	interbedding of sandy layers and seals of finer particles, possible vesicles	2-20	1-5	50	R
Sedimentary (SED)	larger particles at the top, finer particles at the bottom, possible vesicles, frequent curled-up plates	2-50	0-2	72.5	S
Microphytic sedimentary (MSED)	similar to S but more platy in structure and colonised by microphytes as algae and mosses	2-50	4-7	50	P
No crust (BIO)	continuous and evolved forest litter, high termitic porosity	-	25-40	7.5	C

The evident correlation between plants distribution and soil features along the cross-section suggests a feedback effect of vegetation on micro-topography. Models have been proposed (Saco & Moreno-de las Heras, 2013) that consider the effect of solid transport, showing that the effect of abiotic factors as relief, erodibility and soil diffusion are tightly bound

to biotic factors as the protective effect of vegetation on soil in determining vegetation patterns and landforms.

1.2 Water balance in a banded vegetation pattern

Empiric studies have been carried out to measure run-off and soil moisture distribution over tiger bush woodlands (Galle, Ehrmann, & Peugeot, 1999). These studies highlighted the huge difference in run-off generation rate between bare areas and vegetated stripes.

Rainfall is generally assumed to be uniform over the entire woodland. When rainfall is lower than a threshold, no run-off is generated. Over the threshold, run-off generated over bare areas reaches 54% of the annual precipitated amount, while it only covers 2% of the annual precipitated amount over the upslope border of the thicket and 18% over the downslope border. Run-off generated over the core of the thicket is negligible (~1%). This result is caused by two main reasons: firstly, the infiltration coefficient is higher over the vegetated areas, due to the absence of crusts and the higher porosity (also of the type macro-porosity, linked to active termite mounds); secondly, the rainfall threshold for the occurrence of run-off is also higher over vegetated areas.

Soil moisture measurements show that the distribution of the underground water is strongly dependent on the vegetation density. The senescence zone contains a very low amount of water, but still higher than the bare areas, where the water content is generally confined to the first few centimetres. The upslope border of the thicket contains a much higher amount of water. The core of the band contains a huge amount of water, here the infiltration front may progress very deep, up to some meters.

The vegetated pattern behaviours like a source-sink system. The bare areas are a source, as their water content does not increase significantly with ranfall, conversely, they produce run-off which flows downslope, providing the vegetated area an amount of incoming water

which adds up to the rainfall and increases the water content, so vegetated stripes act like a sink.

1.3 Environmental features

The existence of tiger bush has been reported in Africa, Oceania, South America, North America, Asia and Europe. This type of landscape characterizes most of the arid to semi-arid regions, which cover approximately one third of the global emerged surface. The annual rainfall in these regions ranges from 250 to 750 mm/y (Klausmeier, 1999), with few and intense showers concentrated during the two wet seasons. One should notice that the effective rainfall available for vegetation growth is very low in comparison to the precipitated amount due to the high run-off rate typical of tropical storms. In increasingly arid regions, it has been reported that the pattern wavelength increases in time, while the plant density and the band-inter-band ratio decrease. The phenomenon of patterning is not specific to a particular type of vegetation, as instances have been reported of stripes entirely composed by grass, grass and trees, trees and bushes. Neither is it specific to a certain type of soil, as it has been reported in sandy, silty and clayey soils. Self-organized patterns only occur when steepness is gentle and uniform, ranging from 0.2% to 2%, so that overland water flows "as a sheet, and not in incised water channels", as already observed by Macfadyen in 1950 (Macfadyen, 1950). Two types of banded patterns may be identified with regards to the orientation of the bands in relation to the ground slope: either parallel or perpendicular. In the latter case, bands have been reported to migrate upslope with migration speed that depends on the type of vegetation (higher for grass, lower for trees) corresponding to the different duration of the plants generation. Other types of patterns emerge on practically flat ground, in the form of circles, spots, arcs or labyrinths.

When we refer to tiger bush or other types of self-organizes vegetation patterns, underlying hypothesis is that heterogeneity in any climate or soil conditions are absent all over the field, meaning that there is no micro-topographic pattern, such as dunes, or any othe types of patterned reliefs or depressions, and rainfall distribution may also be considered uniform.

1.4 Ecological importance of vegetation patterns

Patterning is a feature of many plant communities, concerning all climates and species. In habitats where more than one species is present, the emergence of patterns is often attributed to the cooperation and competition effects (Greig-Smith, 1979). The ecological implications of vegetation patterns are striking. As it has commonly been accepted that the vegetation composition is strongly affected by its habitat, it appears clear that a deep comprehension of the patterning mechanisms is needed in order to study the environmental features.

Tiger bush belongs to the class of vegetation patterns, and is typically found in one of the most fragile habitats: the transition areas at the border of deserts. Over the last decades, desertification has been a burning issue, especially in the African continent. Desertification and land degradation are led by both natural and anthropic factors, the most important ones being droughts, climate change and inappropriate land-use.

Observing the evolution of a tiger bush is a key part in monitoring the health of the transition areas. It has been observed that after dry periods both the wavelength of the pattern increases and the band-inter-band ratio decreases (Valentin & D'Herbès, 1999). Moreover, evidence has been provided that the bands migration is affected by fluctuating weather regimes (Deblauwe, Couteron, Bogaert, & Barbier, 2012).

Although it is well known that vegetation is heterogeneous within bands, there is a lack of focus on interspecies facilitation/competition mechanisms in banded vegetation patterns. Does the alternation of difference species play a key role in band formation and persistence? What phonological features are responsible in determining plant zonation?

1.5 The role of mathematical modelling in vegetation patterns studies

The study of vegetation patterning has been carried out quite sparsely and in a mostly descriptive way over the decades 1950's-1980's. Postulates were made, for instance, on the importance of the superficial water dynamics in the maintenance of the spatial structure of patterns (Boaler & Hodges, 1964). Aerial photography was the main way to achieve information to speculate on in those years. In the years 1990's, though, a great impulse in vegetation patterns studies were provided by mathematical modelling. The modern computers give the possibility to implement complex models as those implying both temporal and spatial dynamics.

Still, the availability of field data in the years 1990's was limited. A few major experimental campaigns were led, namely HAPEX-Sahel[1] (Goutorbe, et al., 1994) and GCTE-Salt[2] (Menaut, Saint, & Valentin, 1993) as a part of international hydrological and ecological surveys, which together with other more specific surveys, provided punctual *in situ* observations on hydrological phenomena, botanical composition, soil conditions and their interactions, see (Wallace J. S. & Hollwill, 1997), (Seghieri, Galle, Rajot, & Erhmann, 1997), (Galle, Ehrmann, & Peugeot, 1999), (Leprun, 1999), (Thiery, D'Herbes, & Valentin, 1995), (Valentin, D'Herbès, & Poesen, 1999). Although the information provided by these studies was very useful in understanding the mechanisms that take place in a tiger bush, carrying out more

[1] HAPEX-Sahel: Hydrological and Atmospheric Pilot Experiment in Sahel
[2] GCTE-SALT: Global Change Terrestrial Ecosystems-Savane à Long Terme core Project

in situ campaigns was prohibitory due to the imperviousness of the sites, located in inhospitable arid and generally difficult to reach regions. On the other hand, putting in place a physical model is not feasible, because of the large spatial and especially temporal scale of the phenomenon, that is bound to plant life time, and to the very specific climatic conditions that characterize these landscapes.

During the years 2000's, however, a great amount of data became available thanks to the advances in remote sensing. These systematic data series, as satellite images, allow researchers to test new hypothesis via an *a priori* mathematical description, or to fine-tune existent models basing on realistic data. Moreover, climate models outputs are now available which suggest different scenarios in future climate evolution, aside the classical meteorological surveys. Mathematical modeling nowadays has therefore an enhanced importance in the study of vegetation patterns as new experimental acknowledgements are available to compare with the theoretical conclusions.

One of the most important models previously developed for the emergence of vegetation patterns is the one of Klausmeier (Klausmeier, 1999). Analytical expressions for the different aspects of the phenomenon may be derived (Sherratt, 2005), showing for instance that there is a correlation between the pattern wavelength and the travelling waves speed. Cross spectral analysis of aerial photographs and satellite images in different sites provided experimental evidence of this correlation (Deblauwe, Couteron, Bogaert, & Barbier, 2012).

Modelling is used here to test new concepts within the frame of the consolidated theory of Klausmeier (Klausmeier, 1999). The tested concepts mainly concern the coexistence of multiple vegetal species within the vegetated patches of a tiger bush, and the role of each species in the dynamics of the pattern. This issue was suggested by both historical *in situ* observations of floristic zonation, see for instance (Valentin, D'Herbès, & Poesen, 1999), (Seghieri,

Galle, Rajot, & Erhmann, 1997), and recent observations of colonization-retreat dynamics based on cross spectral analysis (Deblauwe, Couteron, Bogaert, & Barbier, 2012).

2 Deterministic models for self-emerging patterns

Vegetation patterns are a worldwide occurrence. We will focus on self-organized vegetation patterns, thus excluding those induced by a pre-existing heterogeneities in external conditions, such as soil substrate or topography. Self-organized vegetation patterns emerge from intrinsic dynamics and interaction between vegetation and environmental conditions, such as limiting resources or climate factors.

In absence of spatial dynamics, the expected configuration of any species in homogeneous external conditions is a corresponding homogeneous state. The appearance of self-organized patterning in absence of external heterogeneities is commonly explained invoking the ability of spatial dynamics of vegetation and resources to destabilize the initial homogeneous state.

May u be any variable representing a species of the system, like a vegetation species or a limiting resource. The kinds of spatial dynamics of vegetation and resources which are typically considered are those of the first and second order, namely:

- ∇u, advective term: differential flow models invoke a difference in the flow rate of the species to explain the emergence of instability. This kind of instability will be described in 2.2
- $\nabla^2 u$, diffusive term: diffusion-driven instability models invoke a difference in the diffusivity of the species to explain the emergence of instability. This kind of instability will be described in 2.1

Another way of considering spatial effects is the use of kernels or cellular automata. Although we are not including these methods in this brief review, we would like to remark that

a qualitative and mathematical correlation between neural models and differential flow instability or diffusion-lead instability models (Borgogno, D'Odorico, Laio, & Ridolfi, 2009).

2.1 Turing-like instability

Instability of non linear dynamic systems of two species may be lead by diffusion if the two species have different diffusivities, as found by Turing in the study of chemical systems (Turing, 1952).

In chemistry and biology, this kind of instability explains a number of patterns, as the spots on a leopard fur coat or the pigment patterns on a shell. Morphogenesis, i.e. the development of pattern and form, is the part of embryology which is mostly concerned by diffusion-lead instability (Murray, 2002). Patterns induced by diffusion are steady state spatially heterogeneous spatial patterns, that means that when the pattern is developed, it remains steady and does not depend on time any more. In biochemistry, the two diffusive species are often referred to as the "activator" and the "inhibitor", but the concept of activation and inhibition may be easily extended to the concepts of "prey" and "predator" when the model is applied to ecology.

May w and n be two diffusive species, respectively the activator and the inhibitor, with coupled local dynamics. The dynamics of the two species are modelled by a pair of partial differential equations involving both diffusion terms and local kinetics h and l, functions of the local values of both variables.

$$\begin{cases} \frac{\partial w}{\partial t} = h(w,n) + \nabla^2 w \\ \frac{\partial n}{\partial t} = l(w,n) + d\nabla^2 n \end{cases}$$

where t is time, d is the ratio of the two species diffusivities d_1 and d_2. All variables are in dimensionless units. ∇^2 is the Laplacian operator. The physical problem may generically be

considered in a tri-dimensional space, but we may as well consider the one-dimensional case, so that space is only defined by an infinite x axis, and $\nabla^2 u = \frac{\partial^2 y}{\partial x^2}$.

The pattern emergence requires (Borgogno, D'Odorico, Laio, & Ridolfi, 2009):

1) the local dynamics to be non-linear;
2) the inhibitor to diffuse faster than the activator.

If the instability is of the diffusion-driven type, then the homogeneous steady state of the system must be linearly stable in absence of diffusion, and linearly unstable in presence of diffusion. In order to find out what conditions must be met to achieve diffusion-lead instability, we need to determine the homogeneous steady state (w_0, n_0) of the system. Homogeneity implies the spatial derivatives to be zero, and steadiness implies the temporal derivatives to be zero. So, (w_0, n_0) is found as the solution of

$$\begin{cases} h(w_0, n_0) = 0 \\ l(w_0, n_0) = 0 \end{cases}$$

For small perturbations around the steady state $u = \begin{pmatrix} w - w_0 \\ n - w_0 \end{pmatrix}$, with $|u| \to 0$, it may be linearized around (w_0, n_0) with a Taylor expansion.

$$\frac{\partial u}{\partial t} = Ju$$

where J is the Jacobian of the system $J = \begin{pmatrix} \frac{\partial h}{\partial w} & \frac{\partial h}{\partial w} \\ \frac{\partial l}{\partial n} & \frac{\partial l}{\partial n} \end{pmatrix}_{(w_0, n_0)} = \begin{pmatrix} h_w & h_n \\ l_w & l_n \end{pmatrix}_{(w_0, n_0)}$

Within the frame of linear stability analysis, the solutions of this system $u(x, t)$ are proportional to $e^{\lambda t}$, where λ is an the eigenvalue of the system. As $u(x, t)$ expresses the temporal evolution of the perturbation impressed to the homogeneous steady state, then (w_0, n_0) is

only linearly stable when the real part of λ is negative, so that $|u| \to 0$ for $t \to \infty$. λ may be found as a solution of

$$|J - \lambda I| = 0$$

where I is the identity matrix. The simple quadratic relation for λ

$$\lambda^2 - (h_w + l_n)\lambda + (h_w l_n - h_n l_w) = 0$$

gives two negative roots for λ when the two conditions are met:

$$h_w + l_n < 0 \quad \text{and} \quad h_w l_n - h_n l_w > 0$$

When diffusion is present, the linearization of the system around the homogeneous steady state with a Taylor expansion gives

$$\frac{\partial u}{\partial t} = Ju + D\nabla^2 u$$

where D is a matrix that contains the diffusion coefficients of the two species $D = \begin{pmatrix} 1 & 0 \\ 0 & d \end{pmatrix}$.

The solutions of this system is a sum of Fourier modes $u(x,t) = U_n e^{\lambda t + inx}$, where λ is an eigenvalue of the system, n is the wave number, and U_n are the Fourier coefficients. λ may be found as a solution of

$$|J - \lambda I - Dn^2| = 0.$$

The characteristic polynomial leads to a relation between eigenvalues and wave numbers which is known as *dispersion relation*.

$$\lambda^2 - (h_w + l_n - dn^2 - n^2)\lambda + (h_w l_n - h_n l_w - dn^2 h_w - n^2 l_n + dn^4) = 0$$

The homogeneous solution (w_0, n_0) is linearly unstable when the real part of at least one eigenvalue λ is positive for some wavenumber $n \neq 0$. This implies the two conditions

$$dh_w + l_n > 0 \quad \text{and} \quad (dh_w + l_n)^2 - 4d(h_w l_n - h_n l_w) > 0$$

The validity of all conditions imposes $d \neq 1$, that means that the two species must have different diffusivity.

The wave number n_{max} corresponding to the maximum positive value of $Re(\lambda)$ is the most unstable mode of the system, meaning that, if the system is unstable, this mode grows faster than the others, so as time passes the oscillation with wavenumber n_{max} prevails on the others and becomes dominating for $t \to \infty$ or until non-linear effects come into play. The final spatial pattern is defined by the wave length relative to n_{max}.

With regard to the amplitude of the oscillation, the linear stability analysis suggests indefinitely growing perturbations when the system is unstable. Nevertheless, as soon as the oscillations grow in amplitude, the initial hypothesis of *small perturbation* ceases to be valid, so that the linearization around the homogeneous steady state of the local kinetics h and l is not an acceptable approximation. To be more precise, in absence of nonlinearities in the local kinetics, the solution found above coincides with the actual solution of the system, giving an indefinitely growing perturbation. So, if we wish to achieve a steady patterned solution, suitable nonlinear terms are needed to provide higher-order terms in the Taylor expansion, which limit the otherwise exponential growth of the perturbation when the amplitude of the perturbation becomes finite.

2.2 Differential flow instability

A second mechanism that causes instability and pattern formation is differential flow. In this case, both species are subject to drift with a different flow rate. The idea behind this

kind of models is quite similar to that of Turing models, but there are two main differences. Firstly, in differential flow instability models, diffusion does not generate symmetry breaking instability, but it plays a crucial role in imposing an upper bound to the range of unstable modes n (Rovinsky & Menzinger, 1992). Secondly, the presence of drift causes the patterns developed by instability to be unsteady, time-dependent patterns; in other words, these patterns are subject to spatial migration in time.

May w and n be two diffusive species, respectively the activator and the inhibitor, the activator being subject to an advective flow, with coupled local dynamics. The dynamics of the two species are modelled by a pair of partial differential equations involving advective terms, diffusion terms and local kinetics h and l, functions of the local values of both variables.

$$\begin{cases} \dfrac{\partial w}{\partial t} = h(w,n) + v\nabla w + \nabla^2 w \\ \dfrac{\partial n}{\partial t} = l(w,n) + d\nabla^2 n \end{cases}$$

where t is time, v is the flow rate of the activator species, d is the ratio of the two species diffusivities d_1 and d_2. All variables are in dimensionless units. ∇ is the gradient and ∇^2 is the Laplacian operator. The physical problem may generically be considered in a tri-dimensional space, but we may as well consider the one-dimensional case, so that space is only defined by an infinite x axis, and $\nabla^2 u = \frac{\partial^2 y}{\partial x^2}$. The advective flow is oriented as the x axis.

If the instability is due to differential flow, then the homogeneous steady state must be linearly stable, as stated in 2.1

The homogeneous steady state (w_0, n_0) is found as the solution of

$$\begin{cases} h(w_0, n_0) = 0 \\ l(w_0, n_0) = 0 \end{cases}$$

For small perturbations around the steady state $u = \begin{pmatrix} w - w_0 \\ n - w_0 \end{pmatrix}$, with $|u| \to 0$, the homogeneous system may be linearized around (w_0, n_0) with a Taylor expansion.

$$\frac{\partial u}{\partial t} = Ju$$

where J is the Jacobian of the system $J = \begin{pmatrix} \frac{\partial h}{\partial w} & \frac{\partial h}{\partial w} \\ \frac{\partial l}{\partial n} & \frac{\partial l}{\partial n} \end{pmatrix}_{(w_0, n_0)} = \begin{pmatrix} h_w & h_n \\ l_w & l_n \end{pmatrix}_{(w_0, n_0)}$

The solutions of this system $u(x,t)$ are proportional to $e^{\lambda t}$, where λ is an the eigenvalue of the system. As $u(x,t)$ expresses the temporal evolution of the perturbation impressed to the homogeneous steady state, then (w_0, n_0) is only linearly stable when the real part of λ is negative, so that $|u| \to 0$ for $t \to \infty$. λ may be found as a solution of

$$|J - \lambda I| = 0$$

where I is the identity matrix.

When differential flow is present, the linearization of the system around the homogeneous steady state with a Taylor expansion gives

$$\frac{\partial u}{\partial t} = Ju + V\nabla u$$

where V is a matrix that contains the flow rates of the two species $V = \begin{pmatrix} v & 0 \\ 0 & 0 \end{pmatrix}$.

The solutions of this system is a sum of Fourier modes $u(x,t) = U_n e^{\lambda t + inx}$, where λ is an the eigenvalue of the system, n is the wave number, and U_n are the Fourier coefficients. λ may be found as a solution of

$$|J - \lambda I - iVn| = 0.$$

where i is the imaginary unit.

Looking at the dispersion relation,

$$\lambda^2 - (h_w + l_n + ivn)\lambda + h_w l_n - h_n l_w + ivnl_n = 0$$

with all derivatives being calculated in (w_0, n_0), one can see that λ is a complex number. The real part of at least one eigenvalue λ must be positive to induce instability, while the imaginary part of the eigenvalue must be non-zero for wave patterns to travel in space. Another important observation is that the λ is a monotically increasing function of the wavenumber n, so it is impossible to determine an upper bound in the range of unstable modes. However, if diffusivity is also considered either for the first or the second species or both species, then an upper bound is imposed in the range of unstable modes (Rovinsky & Menzinger, 1992), so that it a finite value of wave number is determined which gives the dominating mode for $t \to \infty$.

In this case, λ may be found as a solution of

$$|J - \lambda I - iVn - Dn^2| = 0$$

where D is a matrix that contains the diffusion coefficients of the two species $D = \begin{pmatrix} 1 & 0 \\ 0 & d \end{pmatrix}$.

The dispersion relation becomes

$$\lambda^2 - (h_w + l_n + ivn - n^2 - dn^2)\lambda + h_w l_n - h_n l_w + ivnl_n - idvn^3 - n^2 l_n - dn^2 h_w + dn^4 = 0$$

with all derivatives being calculated in (w_0, n_0).

As for the case of Turing instability, suitable nonlinear terms are needed in the local kinetics to prevent the perturbation from growing indefinitely and allow the formation of patterns.

Conversely, the resulting patterns are not steady but progressive. The strict conditions on diffusivities required by the Turing model are not required in presence of advective flow. Nevertheless, diffusion of at least one of the species is needed in order to obtain patterns, which cannot appear if the instability is only induced by drift in absence of diffusion, because there is no upper bound in the range of unstable modes, i.e. the resulting patterns would have infinite wavelength.

2.3 Considering two vegetal species. A three reactants system

In the first paragraphs of this chapter, two kinds of instability due to spatial effects are discussed for the case of a model with two equations and two unknowns. In this case, whatever the form of the model, the matrix of the system is a 2x2 square matrix and the analytical expression for the eigenvalues is a quadratic. Developing an analytical solution is simple and leads to easily comprehensible discussion and conclusions.

For the case of a model with more than two equations, following the analytical path may not be convenient, as the expression found for the system eigenvalues is a at least a cubic. It may be more convenient, instead of developing an analytical expression for the dispersion relation, to solve it numerically and verify the two conditions:

- The homogeneous system is stable to small perturbations around the homogeneous steady state solutions, i.e. the real part of all the system eigenvalues is always negative;
- When a spatial effect (differential diffusion and/or differential flow) is taken into account, the non-homogeneous system is unstable to small perturbations around the homogeneous steady state solutions, i.e. the real part of at least one of the system eigenvalues is positive for some wavenumber $n \neq 0$.

If the two conditions are met, then the instability is effectively due to the spatial effects.

2.4 An algorithm for stability analysis

Let us suppose we wish to represent an ecological dynamic process such as the degeneration of a uniformly vegetated grassland or forest into a *tiger bush*, and that we suppose instability to be due to spatial effects.

Once the model equations are set, and the coefficients are chosen, we need to define a spatial domain, set the initial conditions (and the boundary conditions if the spatial domain is finite), set a suitable simulation time, then we can apply the model and look at the results to establish how well the model does describe the phenomenon.

The above procedure though would probably fail, as it is not granted that the model is able to produce a spatial effect induced instability with a patterned long term steady (or progressive) configuration. The equations we choose, in fact, are formulated on a physical basis, but we need to verify that, from a mathematical point of view, they are apt to produce a stable homogeneous solution and an unstable non-homogenous solution.

It becomes evident that we need an instrument to execute an *a priori* test on the model form, in order to establish whether it does respond to it original purpose or not. Moreover, we may want to determine a range for each parameter that makes the model work as desired. This may be very useful when dealing with ecological phenomena, as the actual values of the parameters are hard to set and always carry a certain amount of uncertainty.

In this section, we present an algorithm that is useful to execute the test on any model. The algorithm is developed in *Matlab* language. It is written for a three equations system, but may be very easily extended to a wider system. We show a real example case, that refers to

the model described in 4.1.1. Different values for the parameters as well as different expressions for functions derivatives and the homogeneous state solutions should be set in the appropriate section.

Algorithm 1: Linear stability analysis of a three equations model.

```
%%% INTRODUCTION %%%


% The purpose of this program is to study the linear sta-
bility of the model.
% The model is a three PDEs system in x and t.
% The variables are w(soil water content) and n1, n2 (bi-
omass density).
% The variables are contained in the vector u=[w n1 n2].
% The variation in time of any variable is equal to a
function of all the variables plus a drift term plus a
diffusion term:
% u,t=F(u)+V*u,x+D*u,xx
% where
% u,t=[w,t n1,t n2,t], F(u)=[l(w,n1,n2) h(w,n1,n2)
g(w,n1,n2)], V=[v 0; 0 0; 0 0], D=[dw 0 0; 0 1 0; 0 0 d]
%%% PARAMETERS %%%


%%% GENERAL %%%
A=400; % kg*m^-2*year^-1, water supply
% K=4.5; % kg*m^-2, Michaelis Menten constant, carrying
capacity
V=50; % m*s^-1, rate at which water flows downhill
Dw=0.5; % m^2*year^-1, water diffusion
C=0.4; % -, inhibition effect of climax species on pio-
neer species

%%% SPECIES 1 %%%
C1=0.5; % -, weight in facilitated infiltration
J1=0.03; %-, yield
R1=100; % m^4*year^-1*kg^-2, root water uptake coeffi-
cient
M1=4; % year^-1, mortality
D1=1; % m^2*year^-1, seed dispersal

%%% SPECIES 2 %%%
C2=0.5; % -, weight in facilitated infiltration
% J2=0.03; %-, yield
R2=1.5; % m^4*year^-1*kg^-2, root water uptake coeffi-
cient
M2=0.04; % year^-1, mortality
D2=05; % m^2*year^-1, seed dispersal
%%% TWO PARAMETERS VARY IN A CYCLE %%%


PARAMETER1=0.001:0.001:0.1;
PARAMETER2=0:0.01:10;

% preallocating for speed
test0=zeros(length(PARAMETER1),length(PARAMETER2));
test1=zeros(length(PARAMETER1),length(PARAMETER2));

for i1=1:length(PARAMETER1)
    J2=PARAMETER1(i1)

    for i2=1:length(PARAMETER2)
        K=PARAMETER2(i2);
```

Introduction describes conventional names for variables, drift coefficients and diffusion coefficients, and the way the different matrixes are built up.

In this section, all the model parameters have to be set, but for the two parameter we choose to study. In this example, the lines in which K and J2 are defined are commented, because we choose to study the linear stability of the system with these two parameters varying in a range.

Two *for* are opened to let the chosen parameters vary in a range. The ranges for parameter 1 and 2 have to be set here in the vectors *PARAMETER1* and *PARAMETER2*. For instance, here we let *J2* and K vary in the range set in *PARAMETER1* and *PARAMETER2* respectively.

Test0 and *test1* matrixes are allocated for speed.

```
%%% NON DIMENSIONAL PARAMETERS %%%


a=R1^(1/2)*M1^(-3/2)*J1*A;
k=R1^(1/2)*M1^(-1/2)*K;
v=M1^(-1/2)*D1^(-1/2)*V;
dw=Dw/D1;
j=J2/J1;
r=R2/R1;
m=M2/M1;
d=D2/D1;
%%% HOMOGENEOUS STEADY STATE %%%

alpha=C+m/(r*j);
n10=a/(1+r*alpha^2)-k/(C1+C2*alpha);
n20=alpha*n10;
w0=1/n10;
%%% JACOBIAN %%%


lw=-n10^2-r*n20^2;
ln1=(C1*a)/(k+C1*n10+C2*n20)-2*n10*w0-
(C1*a*(C1*n10+C2*n20))/(k+C1*n10+C2*n20)^2;
ln2=(C2*a)/(k+C1*n10+C2*n20)-2*n20*r*w0-
(C2*a*(C1*n10+C2*n20))/(k+C1*n10+C2*n20)^2;
hw=n10^2;
hn1=2*n10*w0-1;
hn2=0;
gw=-j*n20*r*(n10-C*n20);
gn1=-C*j*n20*r*w0;
gn2=j*n20*r*w0-m-j*r*w0*(n10-C*n20);

J=[lw ln1 ln2; hw hn1 hn2; gw gn1 gn2];
%%% LINEAR STABILITY OF THE HOMOGENEOUS STEADY STATE SO-
LUTION %%%


EIGJ=real(eig(J));
L0=EIGJ(find(abs(EIGJ)==max(abs(EIGJ))));

if  (w0>0 && n10>0 && n20>0 && max(L0)<0) % test is posi-
tive if eigenvalue is negative
    test0(i1,i2)=1;
else
    test0(i1,i2)=0;
end

%%% LINEAR STABILITY ANALYSIS %%%


N=0:0.01:1; % wave number

if  (w0>0 && n10>0 && n20>0) % the homogeneous steady
state solution does make physically sense and is not
trivial
    L1=zeros(length(N),1); % preallocating for speed
        for j=1:length(N)
            VV=[v 0 0; 0 0 0; 0 0 0]; % matrix of the
flow rates
            DD=[dw 0 0; 0 1 0; 0 0 d]; % matrix of the
diffusivity coefficients
            B=J-1i*N(j)*VV-N(j)^2*DD; % matrix of the
system with dirft and diffusion
            L1(j)=max(real(eig(B))); % finds the maximum
of the real part of the system matrix with drift and dif-
fusion
        end
end


if  (w0>0 && n10>0 && n20>0 && max(L0)<0 && max(L1)>0) %
test is positive if eigenvalue is positive
    test1(i1,i2)=1;
```

All non-dimensional groups of parameters are here calculated. For more details, see 4.3.

The homogeneous steady state is here calculated.

All the partial derivatives of the functions are here calculated. The Jacobian matrix is built up.

This section finds which one of the three eigenvalues of the Jacobian has the largest absolute value. If it is negative, than the homogeneous steady state solution is stable to small perturbations, and the *test0* function is set equal to *1*. Else, the homogeneous steady state solution is unstable to small perturbations, and the *test0* function is set equal to *0*.

This section tests the linear stability of the system when drift and diffusion are added.

The wavenumber varies in a range that is set in the vector *N*.

If the real part of the maximum eigenvalue is negative, than the system is unstable to small perturbations, and the *test1* function is set equal to *1*. Else, the system is stable to small perturbations, and the *test1* function is set equal to *0*.

```
else
    test1(i1,i2)=0;
end
    end

end

%%% PLOT OF THE SOLUTIONS %%%


subplot(2,1,1)
surf(PARAMETER1,PARAMETER2,test0')
shading interp
title('Stability of the homogeneous steady state solu-
tion','FontSize',13,'FontWeight','bold');
xlabel('PARAMETER 1','FontSize',10,'FontWeight','bold');
ylabel('PARAMETER 2','FontSize',10,'FontWeight','bold');
view(2);

subplot(2,1,2)
surf(PARAMETER1,PARAMETER2,test1')
shading interp
title('Instability due to diffusion and drift','Font-
Size',13,'FontWeight','bold');
xlabel('PARAMETER 1','FontSize',10,'FontWeight','bold');
ylabel('PARAMETER 2','FontSize',10,'FontWeight','bold');
view(2);
```

The previously opened *for* cycles are closed.

Plots a subdivided plot. The top half of the plot shows the value of the *test0* function in the plane that is defined by the range of *PARAMETER1* in the *x-axis* and by the range of *PARAMETER2* in the *y-axis*. The bottom half of the plot shows the value of the *test1* function in the plane that is defined by the range of *PARAMETER1* in the *x-axis* and by the range of *PARAMETER2* in the *y-axis*.

For instance, the algorithm with the reported parameters values and the expressions gives

Figure 3 as output image:

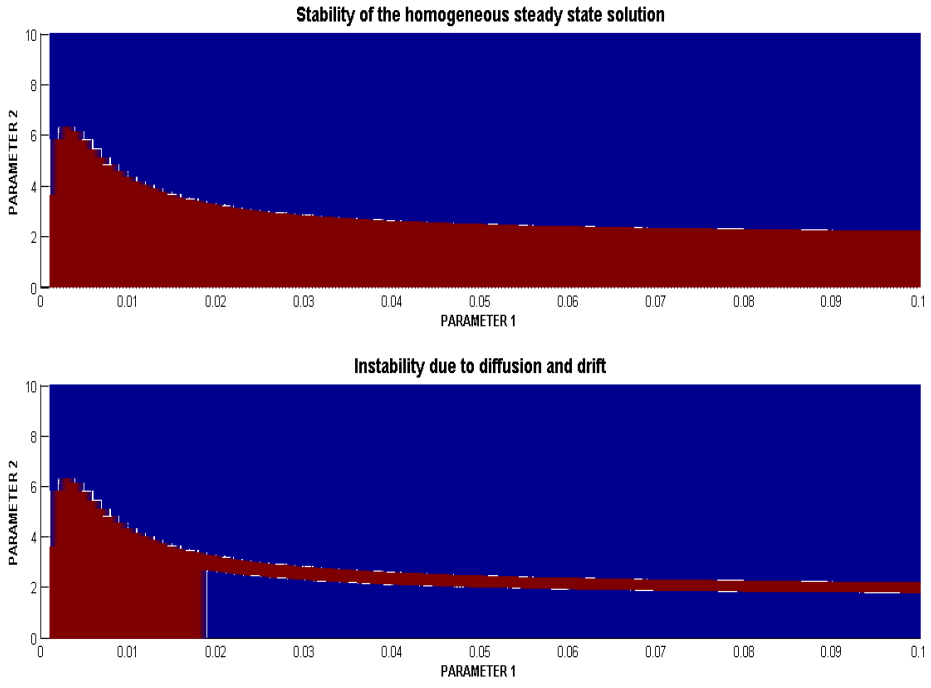

Figure 3: Output of the linear stability analysis algorithm.

The red area in the two parameters plane defines the region of the parameters that give a linearly stable homogeneous steady state solution (top half) and an unstable non-homogeneous system (bottom half).

Once an appropriate set of parameters identified, one may better fine-tune the model by making a third parameter vary in a range. For example, if we set $K=4.2\ kg\ m^2$ and $J_2=0.01$, and let A vary between 0 and $1000\ kg\ m^2/year$, we find (Figure 4) that the real part of the maximum eigenvalue of the system has is maximum for $A=284\ kg\ m^2/year$. Moreover, we may remark that for A cannot go below the $284\ kg\ m^2/year$ threshold as there is no stable homogenous steady state solution, while for $A>284\ kg\ m^2/year$ the value of the real part of the maximum eigenvalue decreases.

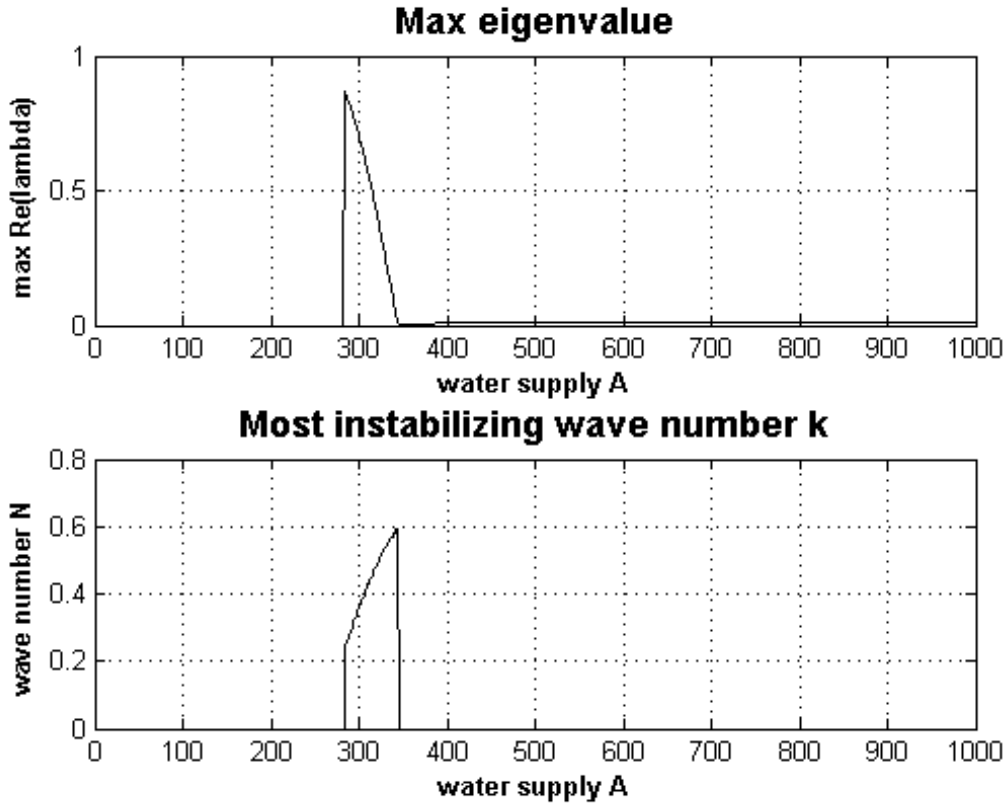

Figure 4: Real part of the maximum eigenvalue for varying values of parameter A.

Once all the parameters set, the model is completely defined. In this case, if we set *A=290 kg m²/year*, we find (Figure 5) that the most unstable wavenumber is *N=0,29*.

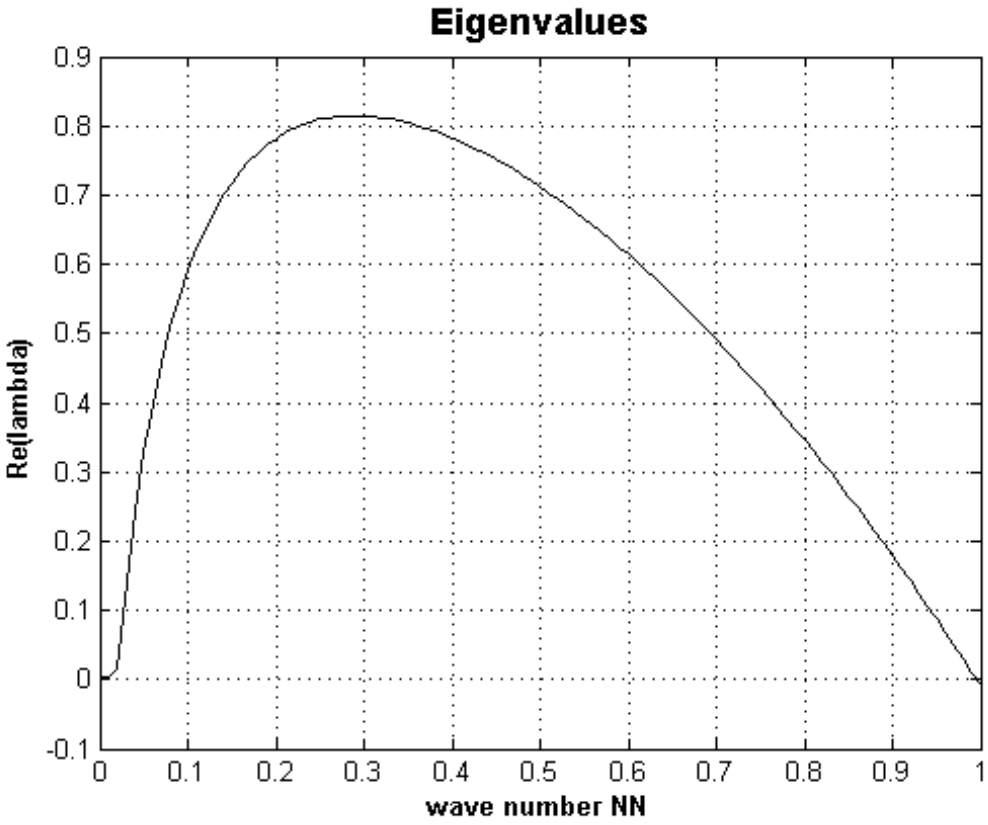

Figure 5: Real part of the maximum parameter of the system versus wavenumber.

3 Klausmeier's model

Our model is based upon the one of Klausmeier (Klausmeier, 1999), which consists of a pair of differential equations for plant biomass (N) and surface water (W), in its one-dimensional form,

$$\begin{cases} \frac{\partial W}{\partial T} = A - LW - RWN^2 + V\frac{\partial W}{\partial X} \\ \frac{\partial N}{\partial T} = JRWN^2 - MN + D\frac{\partial^2 N}{\partial X^2} \end{cases}$$

where T is the time and X is the infinite spatial domain (on hillsides, the soil elevation decreases as X increases).

The first equation represents a water balance where the different contributions to the variation of W are respectively:

- $+A$: water supply, due to uniform rainfall;
- $-LW$: water loss. It is modelled as linear to water with loss coefficient L;
- $-RWN^2$: water uptake by plants. The root water uptake is modelled as proportional to water and to the square of plant biomass with a coefficient R;
- $+V\frac{\partial W}{\partial X}$: water removal due to water flow downhill at uniform speed V.

The second equation represents a plant biomass balance where the different contributions to the variation of N are respectively:

- $+JRWN^2$: plant growth. This term is regarded as proportional to water uptake with a yield coefficient J;
- $-MN$: plant mortality, modeled as linear to the plant biomass itself;
- $+D\frac{\partial^2 W}{\partial X^2}$: plant dispersal, modelled by a diffusion term with diffusion coefficient D.

The units of measurements for variables and parameters are respectively:

Table 2: Units of measurement for variables in K99.

X	m	spatial domain
T	y	temporal domain
W	$\mathrm{kg_{H2O}\ m^{-2}}$	water
N	$\mathrm{kg_{MO}\ m^{-2}}$	plant biomass

Table 3: Units of measurement for parameters in K99.

L	$\mathrm{y^{-1}}$	water loss coefficient
D	$\mathrm{m^2\ y^{-1}}$	seed dispersal coefficient
R	$\mathrm{m^4\ kg_{MO}{}^{-2}\ y^{-1}}$	root uptake coefficient
J	–	yielding coefficient
A	$\mathrm{kg_{H2O}{}^{-2}\ m^{-2}}$	water supply
V	$\mathrm{m\ y^{-1}}$	water flow velocity
M	$\mathrm{y^{-1}}$	plant mortality

K99 can be non-dimensionalized by subsituting the dimensional variables with their corresponding non-dimensional expressions: $X = {M_1}^{-1/2}{D_1}^{1/2}x$, $T = {M_1}^{-1}t$, $W = {R_1}^{-1/2}{M_1}^{1/2}{J_1}^{-1}w$, $N = {R_1}^{-1/2}{M_1}^{1/2}n$.

Simplifying, we obtain the following system.

$$\begin{cases} \dfrac{\partial w}{\partial t} = \boldsymbol{R^{1/2}L^{-3/2}JA} - w\ - w\,n^2 + \boldsymbol{L^{-1/2}D^{-1/2}V}\dfrac{\partial w}{\partial x} \\ \dfrac{\partial n}{\partial T} = w\,n^2 - \boldsymbol{L^{-1}M}n + \dfrac{\partial^2 n}{\partial x^2} + \dfrac{\partial^2 n}{\partial y^2} \end{cases}$$

The remaining groups of dimensional parameters may be substituted by the corresponding non-dimensional parameters: $a = R^{1/2}L^{-3/2}JA$, $v = L^{-1/2}D^{-1/2}V$, $m = L^{-1}M$.

The non-dimensional model results in the following.

$$\begin{cases} \dfrac{\partial w}{\partial t} = a - w\ - w\,n^2 + v\dfrac{\partial w}{\partial x} \\ \dfrac{\partial n}{\partial t} = w\,n^2 - mn + \dfrac{\partial^2 n}{\partial x^2} + \dfrac{\partial^2 n}{\partial y^2} \end{cases}$$

with only three non-dimensional parameters a (water supply), m (plant mortality) and v (water flow rate).

The model of Klausmeier is one of the most used for reproducing the genesis of vegetated bands in scarcity of resources. One of its key strength is its simplicity. Nonetheless, the mathematical form that is attributed to hydrological and biological phenomena such underground water infiltration and the feedback between water and plants by Klausmeier appears not to be in line with the usual forms which are typically assessed in specific literature.

Let us consider the first equation of the system, which is supposed to describe the dynamics of water content. To be relevant in the interaction with plants, the equation should refer specifically to underground water, so that the equation represents a simple balance of underground water content. The incoming water flow A in such a balance may be considered as an infiltration term, albeit infiltration is known to be highly dependent on soil condition. Given a uniform precipitation above a basin, the quantity of water that infiltrates is very low in correspondence to bare, impermeable soils, conversely infiltration is much higher over vegetated, porous soil (Galle, Ehrmann, & Peugeot, 1999). So, as soon as bands of vegetation and inter-band of bare soil are generated, a uniform term for infiltration over the domain does not seem to be suitable any more to represent the actual water supply. The water loss term $-LW$ also appears to have little sense in arid to semi-arid catchments, as it would represent the water table recharge, which may be neglected when compared to the other hydrological phenomena occurring in the microhabitat of a tiger bush. Moreover, in the model of Klausmeier belowground water diffusion is neglected, although diffusion is relevant in vadose zone water dynamics. A last point one should focus when considering the water equation in K99 is the root water uptake by plants. This term is modelled as a quadratic function of the plant biomass N. The quadratic form expresses a strong local facilitation effect in the use of resources (water) by plants. That means, the water uptake is enhanced in

those regions where the plant density is high, while it is less effective in the scarcely vegetated regions. Because of this facilitation effect, plant growth is favoured within the bands while it results ineffective in the inter-band, and the feedback leads to a growing band-inter-band ratio in time. This mathematical form for root water uptake is not used in traditional water balances for cultivated fields, but appears reasonable in arid, inhospitable regions where local cooperation is carried out by plants to best exploit the scarce resources.

The second equation, which is a biomass balance, appears to be more in line with the commonly used mathematical forms for the population dynamics. The plant growth is proportional to the abundance of resources, in this case the root water uptake, though the quadratic form in N is specific to arid regions where local cooperation effects are emphasized, as considered above. This term represents the development of individuals or of groups of plants located in the same bush. The spatial expansion of bushes, due to seed dispersal, is modelled by a diffusion term. Lastly, the typical assumption is made that the biomass loss due to mortality is proportional to the biomass itself.

4 A two plant species model for vegetation patterns

The coexistence of different plant species within vegetated patches in tiger bush patterns were observed by many authors, see for instance (Seghieri, Galle, Rajot, & Erhmann, 1997). The spatial distribution of the different species is not random, but appears to have a correlation with vegetated bands zonation (Valentin, D'Herbès, & Poesen, 1999). More recently, cross spectral analysis provided experimental evidence of particular colonization-retreat dynamics as a response to fluctuating water supply (Deblauwe, Couteron, Bogaert, & Barbier, 2012). These studies suggest that different plant species within a tiger bush have different roles in maintaining the spatial structure of the pattern, and especially in allowing its migration uphill, as a result of their different phenological features and responses to fluctuating water inputs. Nevertheless, as far as we know, there is a lack of focus on interspecies facilitation-competition mechanisms in banded patterns.

The models developed for the emergence of vegetation patterns in arid lands only consider one plant species. On the other hand, coexistence and competition between species has been widely studied in literature, see for instance (Tilman, 1994). Our purpose here is to examine if the consolidated models for coexisting competitive species may be introduced in a vegetation pattern context to realistically explain the observed dynamics.

For this purpose, we base our study on a strongly established model for patterning in arid lands, add an equation for a second plant species and conveniently modify the equations in order to introduce interspecies facilitation-competition effects. The Klausmeier's model is still nowadays one of the most used and established models for explaining the emergence of vegetation patterns in arid lands. It considers the most important mechanisms in pattern formation, namely: the strong synergy between vegetation and water availability which is

emphasized in arid lands, the spatial effects of water flow and plants propagation by dispersal. Moreover, its striking simplicity allows us to introduce a number of modifications. The model is spatially explicit, so that information on the spatial distribution of variables is provided. The partial differential equations of the model may be converted into a finite difference explicit scheme, allowing numerical implementation.

4.1 Considering two coexisting species

A tiger bush may be regarded as a dynamic habitat, as its configuration evolves in time. As observed by many researchers, see for instance (Valentin, D'Herbès, & Poesen, 1999) and recently confirmed by cross spectral analysis of aerial and satellite images (Deblauwe, Couteron, Bogaert, & Barbier, 2012), vegetated bands tend to migrate uphill, thanks to higher water availability due to run-on at the top edge of the bushes. In these former bare areas, only a few plant species have the ability to take root: these plants are said *pioneer species*, and they have the crucial ecological role of preparing the soil for the rooting of other species, said *climax species*.

Pioneer species are usually annual grasses. They are also known as ruderal, opportunistic or r-selected species, where *r* refers to their high colonization rate. Pioneer species are the first to colonize previously inhospitable species, such as the hard impermeable crusts that are formed in the bare inter-band of a tiger bush, because of the adaptations that allow them to break down crusts into soil for other plants to take root. Pioneer plants are said to be fugitive because they are not good at competing for resources, and they are not shade-tolerant: as soon as other plants arrive, pioneer plants would leave the previously colonized sites and migrate to un-colonized new sites.

Climax species are usually perennial trees. They are also known as late seral, late-successional, K-selected or equilibrium species, where *K* refers to their high carrying capacity. Climax species are slower-colonizer, but they have a higher ability to compete for resources, and their seedlings can grow in the shade of their parent trees without suffering of light scarcity. As they assess in one site, they would reach a long term equilibrium as long as the site remains undisturbed. Nevertheless, they are scarcely resilient to any disturbances.

In the optics of studying on a more ecological base the dynamics of bands migration, a deeper level of complexity should be added to the model, in order to examine the dynamics of two different plant species, a pioneer species and a climax species, and the effects of co-operation and competition they put in place. A third equation is therefore added to the system, describing the dynamics of a pioneer species, which is a second order competitor with regard to the first species. The balance of biomass of the first species, of type climax, does not directly depend on the pioneer species biomass, as it is dominant in the competition for resources. On the other hand, the pioneer species biomass growth is inhibited by the presence of climax species biomass, as it suffers of the shading effect and is a worse competitor for resources.

For the two biomass species the equations we propose are so formulated.

$$\begin{cases} \dfrac{\partial N_1}{\partial T} = \boxed{J_1 R_1 g_1(N_1)} - M_1 N_1 + D_1 \dfrac{\partial^2 N_1}{\partial X^2} \\ \dfrac{\partial N_2}{\partial T} = \boxed{J_2 R_2 g_2(N_1, N_2)} - M_2 N_2 + D_2 \dfrac{\partial^2 N_2}{\partial X^2} \end{cases}$$

N_1 represents the climax species biomass, N_2 represents the pioneer species biomass. $g_1(N_1)$ is a general expression for the growth function of the climax species, which does not depend on the pioneer species biomass density but only on its own biomass density. $g_2(N_1, N_2)$ is a general expression for the growth function of the pioneer species, which depends both on its own biomass density and on that of the competitor climax species.

We tested more interspecies interaction models, based on the most established formulations that may be found in literature, and modified them in order to take into account the synergy between water availability and vegetation density that is a key point in Klausmeier's model, as for all the models explaining vegetation patterns emergence.

Some of the tested models are listed in Table 4.

Table 4: Growth functions for the climax and pioneer species in four tested models.

INTERSPECIES COMPETITION MODEL	CLIMAX SPECIES GROWTH FUNCTION $\boxed{J_1 R_1 g_1(N_1)}$	PIONEER SPECIES GROWTH FUNCTION $\boxed{J_2 R_2 g_2(N_1, N_2)}$
K99 with direct competition	$J_1 R_1 W {N_1}^2$	$J_2 R_2 W N_2 (\boldsymbol{N_2 - C N_1})$
T94	$J_1 R_1 W {N_1}^2 \left(1 - \frac{N_1}{K_1}\right)$	$J_2 R_2 W {N_2}^2 \left(\mathbf{1} - \frac{\boldsymbol{N_1}}{\boldsymbol{K_1}} - \frac{\boldsymbol{N_2}}{\boldsymbol{K_2}}\right) - \boldsymbol{W {N_1}^2 \frac{N_1}{K_1} \frac{N_2}{K_2}}$
MM	$J_1 R_1 W {N_1}^2 \frac{\boldsymbol{N_1}}{\boldsymbol{N_1 + K_1}}$	$J_2 R_2 W N_2 (N_2 - C N_1) \frac{\boldsymbol{N_2}}{\boldsymbol{N_2 + K_2}}$
K99 with direct exclusion	$J_1 R_1 W {N_1}^2$	$J_2 R_2 W N_2 (\mathrm{N}_2 - \mathrm{CN}_1)$ with $\boldsymbol{N_2 \leq C N_1}$

Both species are subject to a linear endogen mortality with mortality rate M_1 and M_2 respectively. Seed dispersal is represented by a diffusive term with dispersal coefficientsD_1 and D_2 respectively.

4.1.1 K99 with direct competition

The equation for N_1 is the same equation used in Klausmeier's model, unmodified. The growth term is proportional to the root uptake that the climax species can fulfil (notice that the root uptake is linear in water content and quadratic in biomass quantity, a reasonable assumption in arid climates where the local cooperation effects are particularly effective, see 3). The equation for N_2 is similar to the equation used in Klausmeier's model, but with

a major modification that accounts for the inhibitive effect the climax species has on the pioneer. The growth term is only proportional to the root uptake that the pioneer species can fulfil if the climax species is absent. On the contrary, the presence of climax species individuals reduce the growth of pioneers, and even converses the growth term in a loss term as soon as the quantity of climax plant biomass exceeds the quantity of pioneers.

Appropriate values for parameters were set as reported in Table 5:

Table 5: K99 with direct competition model parameters.

PARAMETER	UNIT OF MEASUREMENT	VALUE	DESCRIPTION
Climax species			
J_1	$-$	0.03	yielding coefficient
R_1	$m^4\ kg_{MO}{}^{-2}\ y^{-1}$	100	root uptake coefficient
M_1	y^{-1}	4	plant mortality
D_1	$m^2\ y^{-1}$	1	seed dispersal coefficient
Pioneer species			
J_2	$-$	0.03	yielding coefficient
R_2	$m^4\ kg_{MO}{}^{-2}\ y^{-1}$	1.5	root uptake coefficient
C	$-$	1	weight of inhibition of species 1 on species 2
M_2	y^{-1}	0.04	plant mortality
D_2	$m^2\ y^{-1}$	0.1	seed dispersal coefficient

4.1.2 T94

The model is based upon the one introduced by Tilman (Tilman, 1994). In Tilman's model, which is spatially implicit, the superior competitor, i.e. species 1, grows as it was living by itself, without being affected by the presence of the inferior competitor. Species 1 colonizes all the sites where it is not present, i.e. both sites that were colonized by pioneers and bare

areas, but with a low colonization rate. Species 2, instead, can only colonize those sites in which neither species 1 or species 2 are present, i.e. only bare areas, but with a higher colonization rate. Moreover, species 2 loses all those sites that are being invaded by species 1. In other words, species 1 can displace species 2, while the contrary is not possible, but as soon as a site becomes bare due to death of the formerly occupying individual, species 2 colonizes it with a higher rate than species 1. In order to adapt Tilman's model to our spatially explicit model, we substituted the fraction of sites occupied by a species with the ratio between that species biomass and its carrying capacity. Finally, synergy between water availability and plant biomass density was considered in the same way as in Klausmeier's model, by multiplying the growth function by a linear function of water availability.

Appropriate values for parameters were set as reported in Table 6:

Table 6: T94 model parameters.

PARAMETER	UNIT OF MEASUREMENT	VALUE	DESCRIPTION
Climax species			
J_1	$-$	0.03	yielding coefficient
R_1	$m^4\ kg_{MO}^{-2}\ y^{-1}$	100	root uptake coefficient
K_1	$kg\ m^{-2}$	2	carrying capacity
M_1	y^{-1}	4	plant mortality
D_1	$m^2\ y^{-1}$	1	seed dispersal coefficient
Pioneer species			
J_2	$-$	0.03	yielding coefficient
R_2	$m^4\ kg_{MO}^{-2}\ y^{-1}$	1.5	root uptake coefficient
K_2	$kg\ m^{-2}$	4	carrying capacity
M_2	y^{-1}	0.04	plant mortality
D_2	$m^2\ y^{-1}$	0.1	seed dispersal coefficient

4.1.3 MM

The model is based upon model 1 (*K99 with direct competition*), but we use a Michaelis-Menten kinetics (Murray, 2002) (Michaelis & Menten, 1913) where the saturation constant is the growth function.

4.1.4 K99 with direct exclusion

The model is based upon model 1 (*K99 with direct competition*), but we add a limitation to the maximum pioneer species biomass density.

4.2 A more hydraulically based equation for water

The equation we propose for the water balance is based upon the one used by Klausmeier, but is meant to be more realistic, although maintaining a certain simplicity. The variable W is meant to represent explicitly the underground water content.

Infiltration is here considered analogous to a catalytic reaction where water quantity is the product and plant biomass is the substrate. We use a Michaelis-Menten kinetics (Murray, 2002) (Michaelis & Menten, 1913) where the saturation constant is the annual water supply; the concentration of the substrate is a weighted average of the two species biomass N_1 and N_2, with weights C_1 and C_2. Water uptake by the two species is expressed in the same way as in Klausmeier's model, i.e. a function which is linear in water content W and quadratic in plant biomass. The two plant species have different water uptake coefficients though. Any other local water loss term is ignored, as in scarcity of resources it may be assumed that all water which infiltrates is up-taken by plants. The assumption seems correct as infiltration does not occur over the bare areas while it is facilitated by plants over vegetated areas. This is equivalent to neglecting water table recharge.

Water is subject to an advective flow with rate V. The flow is oriented conversely to the x axis. Differently from Klausmeier's model, water is also subject to diffusion with diffusion coefficient D_w.

In the end, the equation we propose for underground water content is so formulated.

$$\frac{\partial W}{\partial T} = A\frac{(C_1N_1 + C_2N_2)}{(C_1N_1 + C_2N_2) + K} - R_1 W {N_1}^2 - R_2 W {N_2}^2 + V\frac{\partial W}{\partial X} + D_w\frac{\partial^2 W}{\partial X^2}$$

Coupling with biomass quantity is present in both the infiltration term and the uptake term. With regard to infiltration, the smallest the total biomass, the lowest the infiltration. If the total biomass is equal to the half-saturation constant K, then the infiltration rate is equal to half the mean annual water supply. If total biomass is much higher than the half-saturation constant K, then the infiltration rate tends to the mean annual water supply. A is the mean annual water supply.

Appropriate values for parameters were set as reported in Table 7:

Table 7: Parameters for water.

PARAMETER	UNIT OF MEASUREMENT	VALUE	DESCRIPTION
A	$kg_{H2O}{}^{-2}\ m^{-2}\ y^{-1}$	350	water supply
K	$kg\ m^{-2}$	3	Michaelis-Menten constant
V	$m\ y^{-1}$	50	water flow velocity
D_W	$m^2\ y^{-1}$	0.5	water diffusivity
C_1	–	0.5	weight of species 1 on facilitated infiltration
C_2	–	0.5	weight of species 2 on facilitated infiltration

4.3 Numerical solution

We pursued a numerical solution of the models in their non-dimensional form by approximating the temporal and spatial derivatives with a finite differences scheme.

As an example, we report the procedure we used for the first model tested (*K99 with direct competition*) below, but we would like to remark that the procedure is analogous for all models.

Let us consider the first model tested, namely *K99 with direct competition*, the interspecies interactions for which are described in 4.1.1.

Putting the three equations together, the model is

$$\begin{cases} \dfrac{\partial W}{\partial T} = A\dfrac{(C_1N_1 + C_2N_2)}{(C_1N_1 + C_2N_2) + K} - R_1 W {N_1}^2 - R_2 W {N_2}^2 + V\dfrac{\partial W}{\partial X} + D_w\dfrac{\partial^2 W}{\partial X^2} \\ \dfrac{\partial N_1}{\partial T} = J_1 R_1 W {N_1}^2 - M_1 N_1 + D_1\dfrac{\partial^2 N_1}{\partial X^2} \\ \dfrac{\partial N_2}{\partial T} = J_2 R_2 W N_2 (N_2 - CN_1) - M_2 N_2 + D_2\dfrac{\partial^2 N_2}{\partial X^2} \end{cases}$$

The units of measurements of variables are reported in Table *8*:

Table 8: Units of measurement for variables in the new model.

VARIABLE	UNIT OF MEASUREMENT	DESCRIPTION
X	m	spatial domain
T	y	temporal domain
W	kg m^{-2}	underground water content
N_1	kg m^{-2}	plant biomass density species 1
N_2	kg m^{-2}	plant biomass density species 2

The units of measurements of parameters are reported in Table *9*:

Table 9: Units of measurement for variables in the new model.

PARAMETER	UNIT OF MEASUREMENT	DESCRIPTION
A	$\mathrm{kg}^{-2}\ \mathrm{m}^{-2}\ \mathrm{y}^{-1}$	water supply
K	$\mathrm{kg\,m}^{-2}$	Michaelis-Menten constant
V	$\mathrm{m}\ \mathrm{y}^{-1}$	water flow velocity
D_w	$\mathrm{m}^2\ \mathrm{y}^{-1}$	water diffusivity
D_1, D_2	$\mathrm{m}^2\ \mathrm{y}^{-1}$	seed dispersal coefficient
R_1, R_2	$\mathrm{m}^4\ \mathrm{kg}^{-2}\ \mathrm{y}^{-1}$	root uptake coefficient
J_1, J_2	–	yielding coefficient
M_1, M_2	y^{-1}	plant mortality
C_1, C_2	–	weight of each species on facilitated infiltration
C	–	weight of inhibition of species 1 on species 2

The dimensional variables may be substituted with their corresponding non-dimensional expressions: $X = {M_1}^{-1/2}{D_1}^{1/2}x, T = {M_1}^{-1}t, W = {R_1}^{-1/2}{M_1}^{1/2}{J_1}^{-1}w, N = {R_1}^{-1/2}{M_1}^{1/2}n.$

Simplifying, we obtain the following system.

$$\begin{cases} \frac{\partial \mathrm{w}}{\partial \mathrm{t}} = {\mathrm{R}_1}^{1/2}{\mathrm{M}_1}^{-3/2}\mathrm{J}_1\mathrm{A}\frac{(\mathrm{C}_1\mathrm{n}_1 + \mathrm{C}_2\mathrm{n}_2)}{(\mathrm{C}_1\mathrm{n}_1 + \mathrm{C}_2\mathrm{n}_2) + {\mathrm{R}_1}^{1/2}{\mathrm{M}_1}^{-1/2}\mathrm{K}} - \mathrm{w}{\mathrm{n}_1}^2 - {\mathrm{R}_1}^{-1}\mathrm{R}_2\mathrm{w}{\mathrm{n}_2}^2 + {\mathrm{M}_1}^{-1/2}{\mathrm{D}_1}^{-1/2}\mathrm{V}\frac{\partial \mathrm{w}}{\partial \mathrm{x}} + {\mathrm{D}_1}^{-1}\mathrm{D}_\mathrm{w}\frac{\partial^2 \mathrm{w}}{\partial \mathrm{x}^2} \\ \frac{\partial \mathrm{n}_1}{\partial \mathrm{t}} = \mathrm{w}{\mathrm{n}_1}^2 - \mathrm{n}_1 + \frac{\partial^2 \mathrm{n}_1}{\partial \mathrm{x}^2} \\ \frac{\partial \mathrm{n}_2}{\partial \mathrm{t}} = {\mathrm{J}_1}^{-1}\mathrm{J}_2{\mathrm{R}_1}^{-1}\mathrm{R}_2\mathrm{w}\mathrm{n}_2(\mathrm{n}_2 - \mathrm{C}\mathrm{n}_1) - {\mathrm{M}_1}^{-1}\mathrm{M}_2\mathrm{n}_2 + {\mathrm{D}_1}^{-1}\mathrm{D}_2\frac{\partial^2 \mathrm{n}_2}{\partial \mathrm{x}^2} \end{cases}$$

The remaining groups of dimensional parameters may be substituted by the corresponding non-dimensional parameters: $a = {R_1}^{1/2}{M_1}^{-3/2}J_1A, k = {R_1}^{1/2}{M_1}^{-1/2}K, v = {M_1}^{-1/2}{D_1}^{-1/2}V,$ $d_w = {D_1}^{-1}D_w, j = {J_1}^{-1}J_2, r = {R_1}^{-1}R_2, m = {M_1}^{-1}M_2, d = {D_1}^{-1}D_2.$

The non-dimensional model results in the following.

$$\begin{cases} \dfrac{\partial w}{\partial t} = a\dfrac{(C_1 n_1 + C_2 n_2)}{(C_1 n_1 + C_2 n_2) + k} - w{n_1}^2 - rw{n_2}^2 + v\dfrac{\partial w}{\partial x} + d_w \dfrac{\partial^2 w}{\partial x^2} \\ \dfrac{\partial n_1}{\partial t} = w{n_1}^2 - n_1 + \dfrac{\partial^2 n_1}{\partial x^2} \\ \dfrac{\partial n_2}{\partial t} = jrwn_2(n_2 - Cn_1) - mn_2 + {D_1}^{-1} D_2 \dfrac{\partial^2 n_2}{\partial x^2} \end{cases}$$

Basing on the parameter values set in 4.1.1, the dimensionless groups values are reported in Table 10, and the variables scaling factors are reported in Table 11.

Table 10: Non-dimensional parameter groups.

NON-DIMENSIONAL PARAMETER	DESCRIPTION	VALUE
a	non dimensional water supply	13.1250
k	non dimensional Michaelis-Menten constant for water	15
v	non dimensional flow rate	25
d_w	ratio between water diffusivity and climax species diffusivity	0.5
j	ratio between climax species yielding coefficient and pioneer species yielding coefficient	1
r	ratio between climax species root uptake coefficient and pioneer species root uptake coefficient	0.0151
m	ratio between climax species mortality and pioneer species mortality	0.01
d	ratio between climax species diffusivity and pioneer species diffusivity	0.01

Table 11: Variables scaling factors.

VARIABLE	SCALING FACTOR
$X:x$	1:2
$T:t$	1:4
$W:w$	1:0.15
$N_1:n_1$	1:5
$N_2:n_2$	1:5

The model has one non trivial homogeneous steady state solution $(w_0,\ n_{10},\ n_{20})$. Let us name $\alpha = C + \frac{m}{jr}$, the homogeneous state solution is:

$$n_{10} = \frac{a}{(1+r\alpha^2)} - \frac{k}{(C_1+C_2\alpha)};\ n_{20} = \alpha n_{10};\ w_0 = \frac{1}{n_{10}}.$$

Basing on the parameter values set in 4.1.1, the value of the homogeneous steady state solution is $\alpha = 1.6667$, $n_{10} = 1.3500$, $n_{20} = 2.2500$, $w_0 = 0.7407$.

The model can be approximated with a finite differences scheme. We choose a centred scheme. Let us introduce a discrete spatial domain, with a number of points spaced by the spatial step dx. A discrete temporal domain is also introduced, with time step dt. Say it the time index and i the space index.

$$\begin{cases} \frac{w_i^{it+1} - w_i^{it}}{dt} = a\frac{\left(C_1 {n_1}_i^{it} + C_2 {n_2}_i^{it}\right)}{\left(C_1 {n_1}_i^{it} + C_2 {n_2}_i^{it}\right) + k} - w_i^{it} {n_1}_i^{it\,2} - r w_i^{it} {n_2}_i^{it\,2} + v\frac{w_{i+1}^{it} - w_{i-1}^{it}}{2dx} + d_w\frac{w_{i+1}^{it} - 2w_i^{it} + w_{i-1}^{it}}{dx^2} \\ \frac{{n_1}_i^{it+1} - {n_1}_i^{it}}{dt} = w_i^{it} {n_1}_i^{it\,2} - {n_1}_i^{it} + \frac{{n_1}_{i+1}^{it} - 2{n_1}_i^{it} + {n_1}_{i-1}^{it}}{dx^2} \\ \frac{{n_2}_i^{it+1} - {n_2}_i^{it}}{dt} = jr w_i^{it} {n_2}_i^{it}\left({n_2}_i^{it} - C{n_1}_i^{it}\right) - m{n_2}_i^{it} + d\frac{{n_2}_{i+1}^{it} - 2{n_2}_i^{it} + {n_2}_{i-1}^{it}}{dx^2} \end{cases}$$

We obtain the explicit scheme:

$$\begin{cases} w_i^{it+1} = w_i^{it} + dt\left[a\frac{\left(C_1 {n_1}_i^{it} + C_2 {n_2}_i^{it}\right)}{\left(C_1 {n_1}_i^{it} + C_2 {n_2}_i^{it}\right) + k} - w_i^{it} {n_1}_i^{it\,2} - r w_i^{it} {n_2}_i^{it\,2} + v\frac{w_{i+1}^{it} - w_{i-1}^{it}}{2dx} + d_w\frac{w_{i+1}^{it} - 2w_i^{it} + w_{i-1}^{it}}{dx^2}\right] \\ {n_1}_i^{it+1} = {n_1}_i^{it} + dt\left[w_i^{it} {n_1}_i^{it\,2} - {n_1}_i^{it} + \frac{{n_1}_{i+1}^{it} - 2{n_1}_i^{it} + {n_1}_{i-1}^{it}}{dx^2}\right] \\ {n_2}_i^{it+1} = {n_2}_i^{it} + dt\left[jr w_i^{it} {n_2}_i^{it}\left({n_2}_i^{it} - C{n_1}_i^{it}\right) - m{n_2}_i^{it} + d\frac{{n_2}_{i+1}^{it} - 2{n_2}_i^{it} + {n_2}_{i-1}^{it}}{dx^2}\right] \end{cases}$$

The finite differences scheme allows us to calculate the state of the system at any point of the spatial domain at any desired moment in time, provided we choose a sufficiently small time step and spatial step. Basing on the diffusivity and flow rate values, appropriate time step and spatial step were fixed respectively at $dT = \frac{1}{366*12} years \cong 2hours$, $dX = 0.5\ m$.

Initial conditions and boundary conditions are needed. Because the natural phenomenon we are trying to imitate, i.e. the genesis and evolution of a tiger bush, does not depend on external heterogeneities, we choose to use cylindrical boundary conditions. The extension of our spatial domain is set to $50\ m$. Before the emergence of patterns, we suppose that the domain is characterized by a uniform underground water distribution and a uniform vegetation cover, with water content and biomass density assuming their homogeneous steady state values, in order to avoid biases due to any initial heterogeneity.

A small random perturbation is added to the initial homogeneous distribution. If the perturbation is sufficiently small, the linear stability of the system may be determined by studying the sign of the dominating eigenvalue. If the sign is negative, then the perturbation is attenuated in time, and after a sufficiently long simulation time the value of the variables turns back to the homogeneous steady state all over the spatial domain. Else, the perturbation increases in time. In a linear system, a perturbation would increase indefinitely in time, but in presence of non-linearities and coupling, patterns may emerge, in the form of a wave train either steady or progressive. As time passes, the most instable mode prevails and for long simulation times it remains the only noticeable one.

5 Results and discussion

We show here the results of two of the models we implemented in order to take into account multispecies interaction within the frame of vegetation patterns models. We focus on the models K99 with direct competition and T94. Other models based on Klausmeier's growth function give similar results to the first one.

5.1 Homogenous steady state solution

The homogeneous steady state solution may be found, either analytically or numerically, for the two models and is reported in Table 12.

Table 12: Homogeneous steady state solutions.

INTERSPECIES COMPETITION MODEL	HOMOGENEOUS STEADY STATE SOLUTION		
	n_{10}	n_{20}	w_0
K99 with direct competition	1.3500	2.2500	0.7407
T94	1.3799	3.1842	0.8444

In both cases, which are characterized by similar parameters, one non trivial, non-negative, linearly stable homogeneous state solution exists. In the homogeneous steady state solution, the two competitive species may coexist, the pioneer species biomass being higher than the climax species biomass thanks to the minor water and resources demand.

5.2 Pattern configuration after a 25 years simulation

We show here the spatial configuration of patterns after a 25 years simulation time. In the top half of the graphs, the two species biomass densities in their non-dimensional form are plotted versus the spatial domain in its dimensional form. Black points represent the climax species biomass density, while circles represent the pioneer species biomass density. In the

bottom half of the graphs, water availability in its non-dimensional form is plotted versus the spatial domain in its dimensional form.

5.2.1 K99 with direct competition

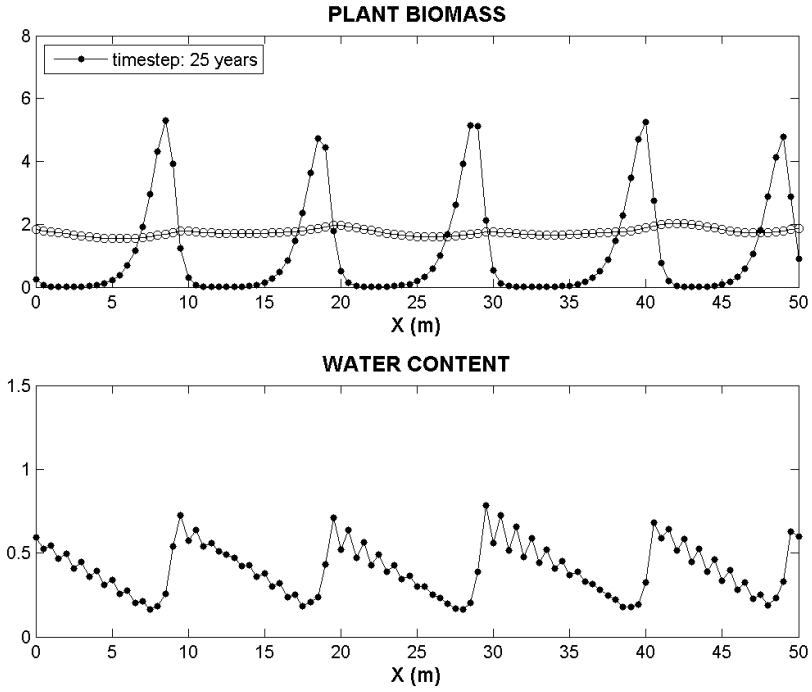

Figure 6: K99 with direct competition. Patterns configuration after a 25 years simulation time.

A pattern is clearly noticeable in form of a succession of bands. The pattern is similar to a wave with wavelength *10 m.* The form of the wave is different for the three variables. However, the three waves present peaks and troughs in correlated positions. Species 1 exhibits very narrow bands and completely bare inter-bands. Species 2 bands are slightly noticeable, with a very low peak and a wide shape, and non-bare inter-band. When interpreting the plot, one should remark that water flows from the right-side to the left-side, i.e., if the ground is on a slope, the ground level decreases from the right part to the left part of the domain. If we look at the pattern upslope to downslope, we are able to see that when species 1 starts to increase in density, the species 2 decreases because of the inhibition effect: after

species 2 reaches a peak and starts decreasing its biomass, species 1 continues increasing and reaches its peak more downslope. This part may be thought as the core of the thicket. When species 1 reaches high levels of density, water content is subject to a sudden decrease, because of the high root uptake rate. As an immediate feed-back effect, species 1 biomass decreases, and so does species 2, but with a lower rate because of the interrupted inhibition. This zone corresponds to the senescence zone. Eventually, species 1 density becomes null. Water content is slowly able to increase due to the very low root uptake. This zone corresponds to the bare inter-band. Thanks to the ceased inhibition by species 1 and to the increasing water abundance, species 2 is able to increase. This zone is the pioneer zone: the pioneer species starts to colonize but there are not yet enough resources for the climax species to develop.

5.2.2 T94

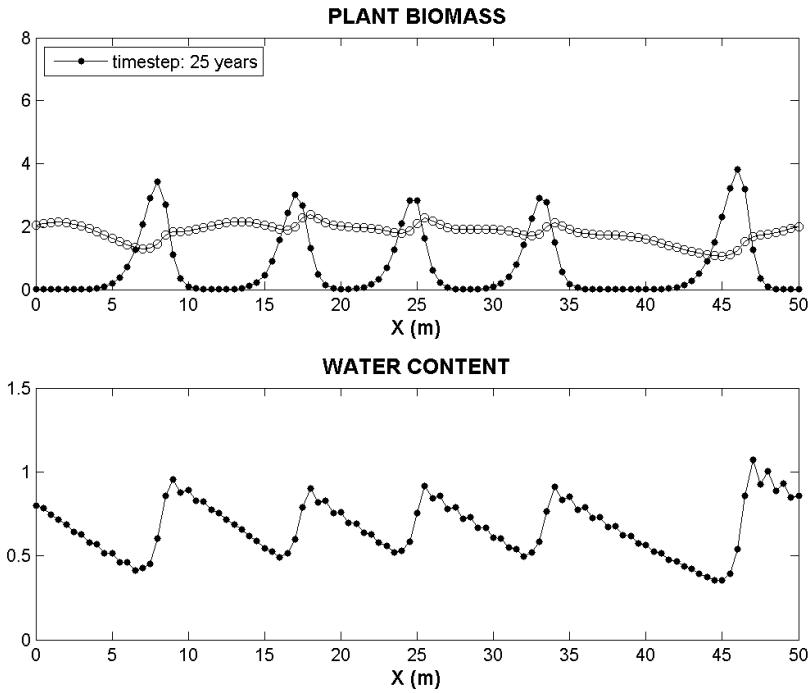

Figure 7: T94. Patterns configuration after a 25 years simulation time.

A pattern is clearly noticeable in form of a succession of bands. The pattern is similar to a quite irregular wave with average wavelength *10 m.* The form of the wave is different for the three variables. However, the three waves present peaks and troughs in correlated positions. Species 1 exhibits very narrow bands and completely bare inter-bands. Species 2 bands are more definite than for *K99 with direct competition*, but still their peak is not as high as the one of species 1, and the bands are large with non-bare inter-band. When interpreting the plot, one should remark that water flows from the right-side to the left-side, i.e., if the ground is on a slope, the ground level decreases from the right part to the left part of the domain. If we look at the pattern upslope to downslope, we are able to see that when species 1 starts to increase in density, the species 2 decreases because of the inhibition effect: after species 2 reaches a peak and starts decreasing its biomass, species 1 continues increasing and reaches its peak more downslope. This part may be thought as the core of the thicket. When species 1 reaches high levels of density, water content is subject to a sudden decrease, because of the high root uptake rate. As an immediate feed-back effect, species 1 biomass decreases, and so does species 2, but with a lower rate because of the interrupted inhibition. This zone corresponds to the senescence zone. Eventually, species 1 density becomes null. Water content is slowly able to increase due to the very low root uptake. This zone corresponds to the bare inter-band. Thanks to the ceased inhibition by species 1 and to the increasing water abundance, species 2 is able to increase. This zone is the pioneer zone: the pioneer species starts to colonize but there are not yet enough resources for the climax species to develop.

5.3 Patterns evolution

We show here the temporal evolution of patterns configuration over a 100 years simulation time. We focus on the first model *K99 with direct competition*. A similar behavior of the patterns configuration was observed for all models. In the top half of the graphs, the two

species biomass densities in their non-dimensional form are plotted versus the spatial domain in its dimensional form. Black points represent the climax species biomass density, while circles represent the pioneer species biomass density. In the bottom half of the graphs, water availability in its non-dimensional form is plotted versus the spatial domain in its dimensional form.

5.3.1 K99 with direct competition

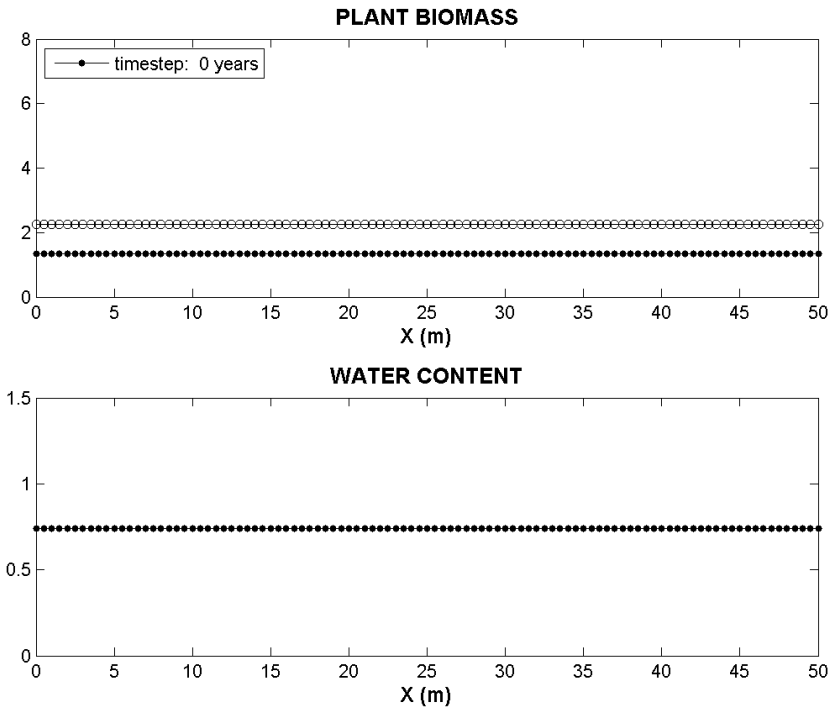

Figure 8: K99 with direct competition. Patterns configuration at initial conditions.

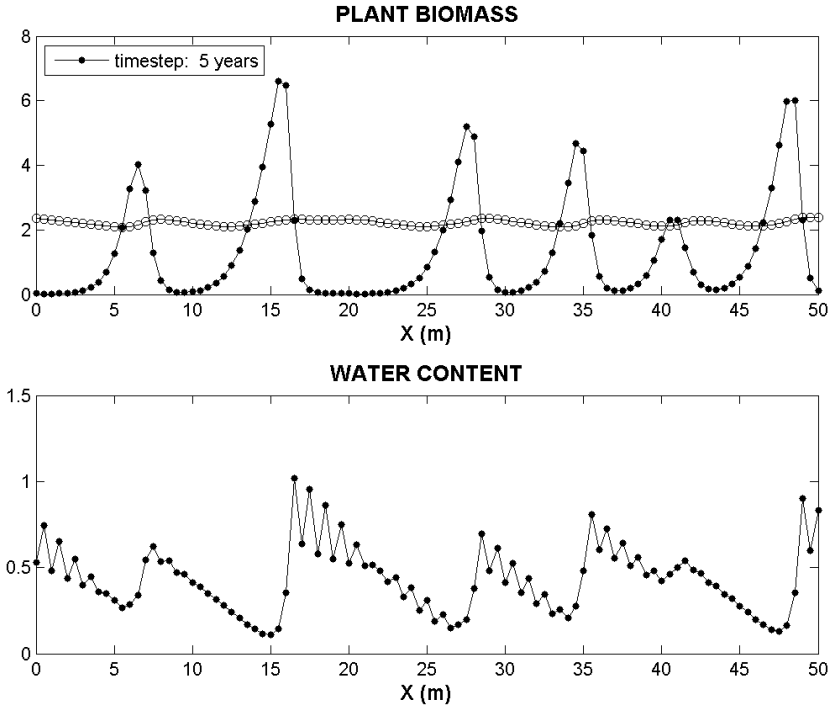

Figure 9: K99 with direct competition. Patterns configuration after a 5 years simulation time.

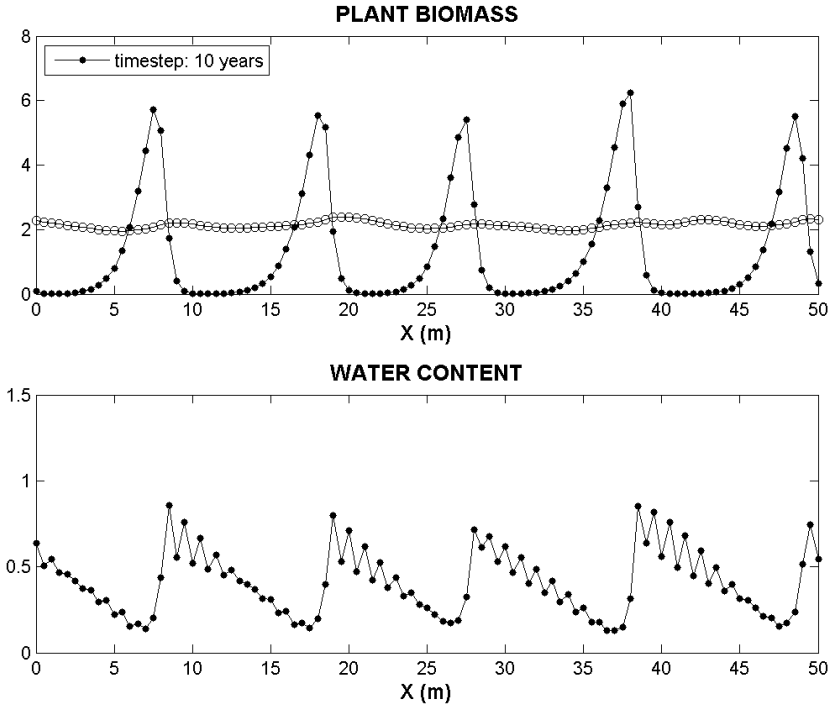

Figure 10: K99 with direct competition. Patterns configuration after a 10 years simulation time.

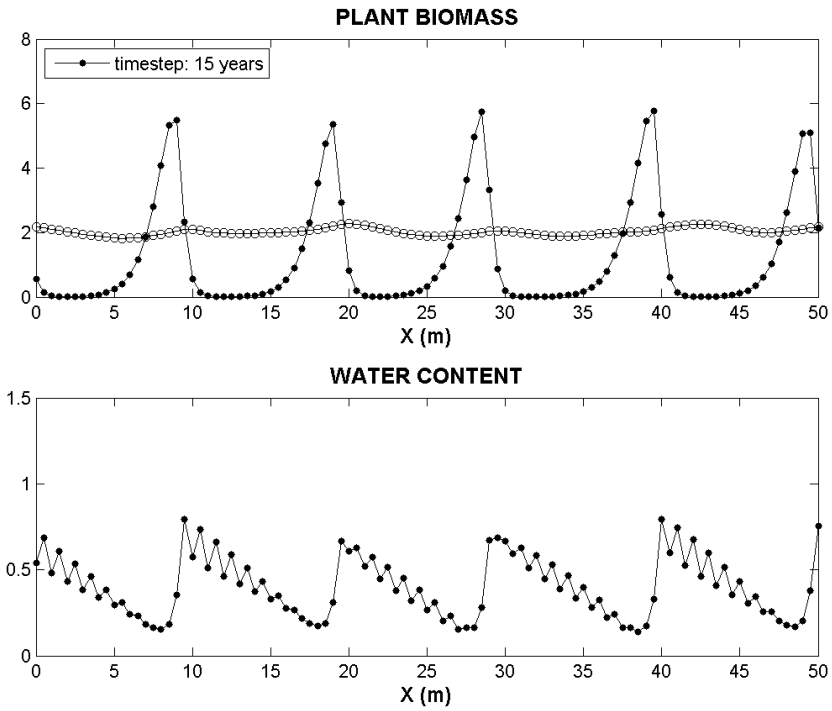

Figure 11: K99 with direct competition. Patterns configuration after a 15 years simulation time.

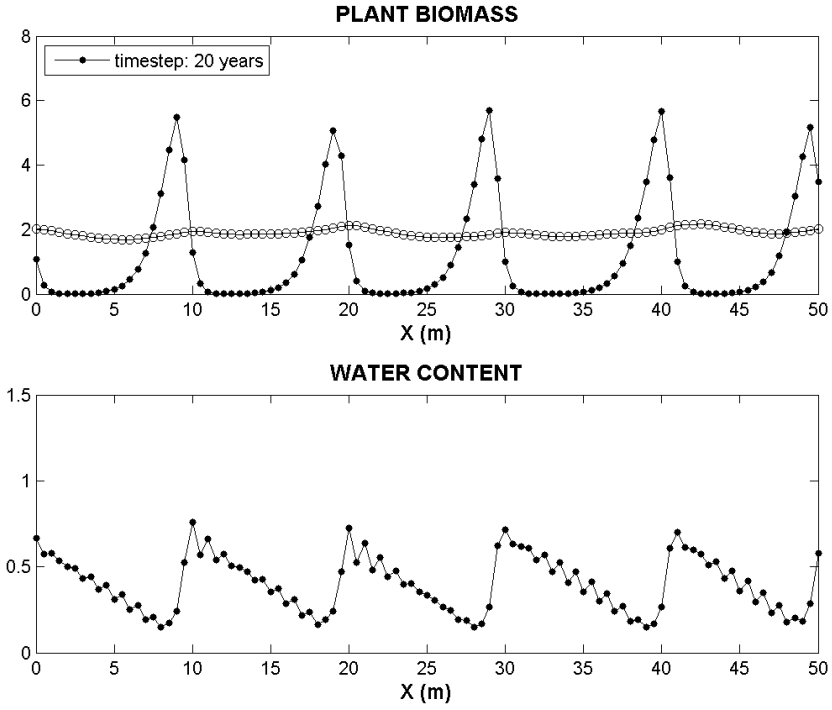

Figure 12: K99 with direct competition. Patterns configuration after a 20 years simulation time.

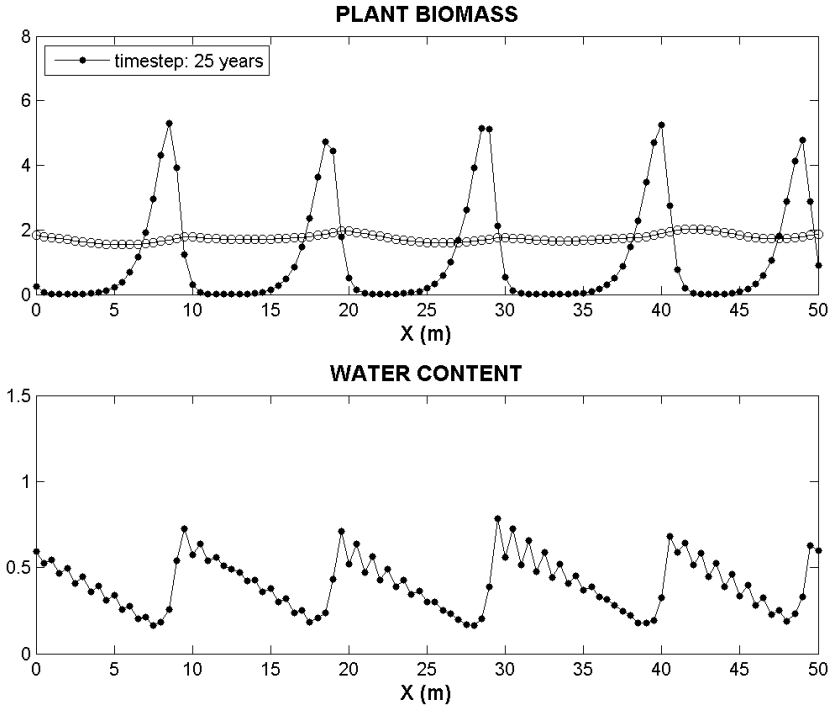

Figure 13: K99 with direct competition. Patterns configuration after a 25 years simulation time.

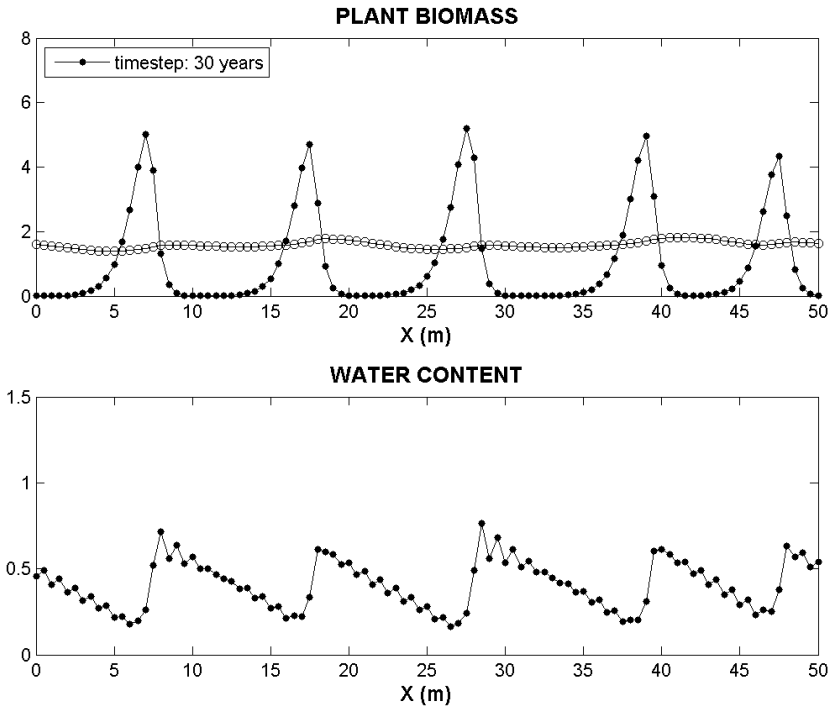

Figure 14: K99 with direct competition. Patterns configuration after a 30 years simulation time.

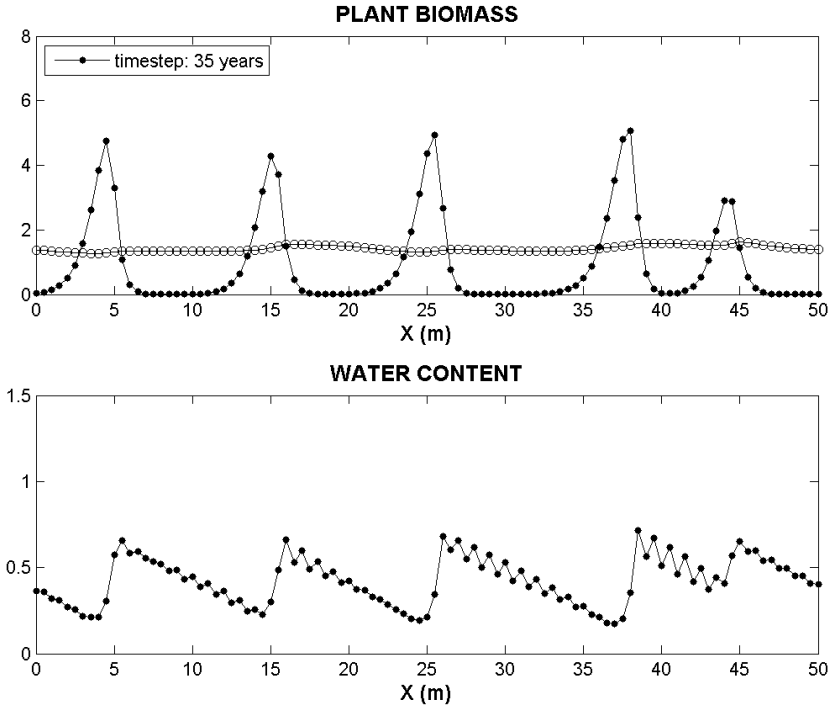

Figure 15: K99 with direct competition. Patterns configuration after a 35 years simulation time.

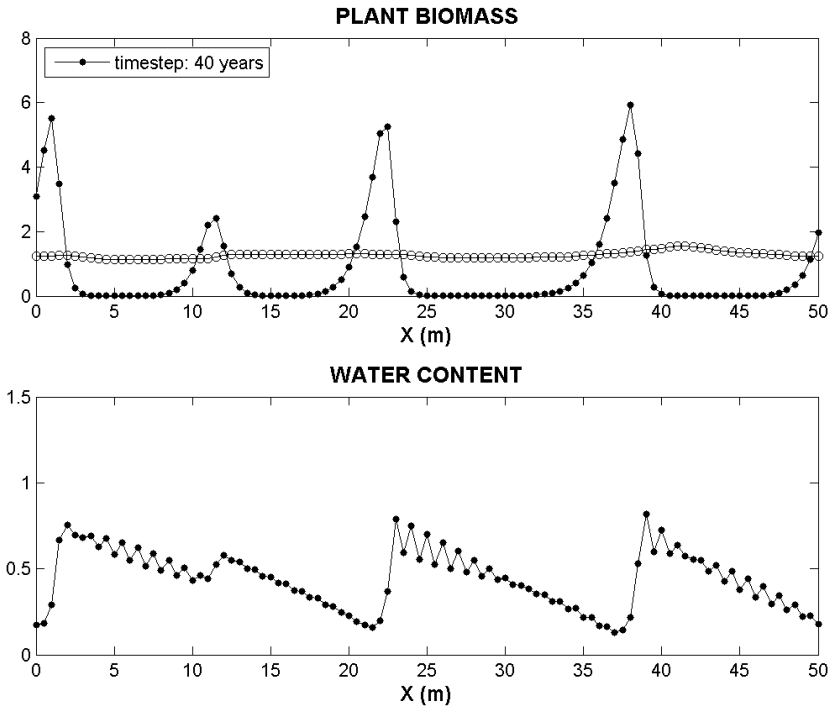

Figure 16:K99 with direct competition. Patterns configuration after a 40 years simulation time.

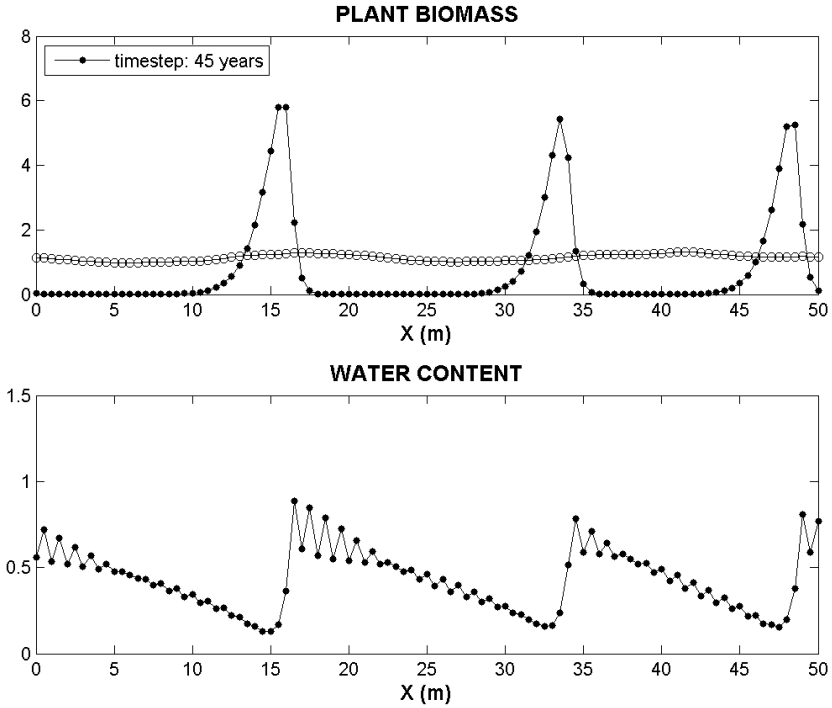

Figure 17: K99 with direct competition. Patterns configuration after a 45 years simulation time.

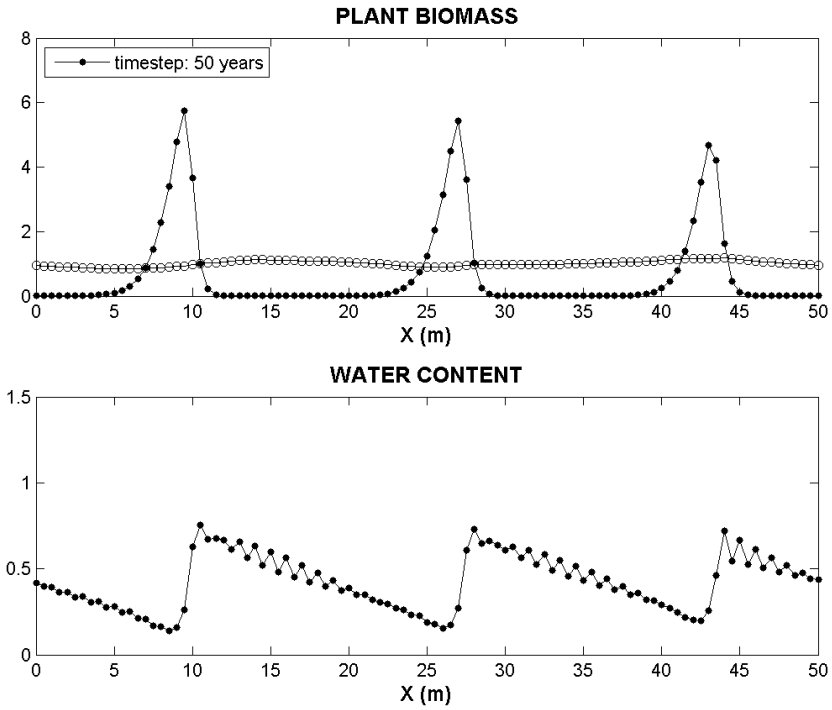

Figure 18: K99 with direct competition. Patterns configuration after a 50 years simulation time.

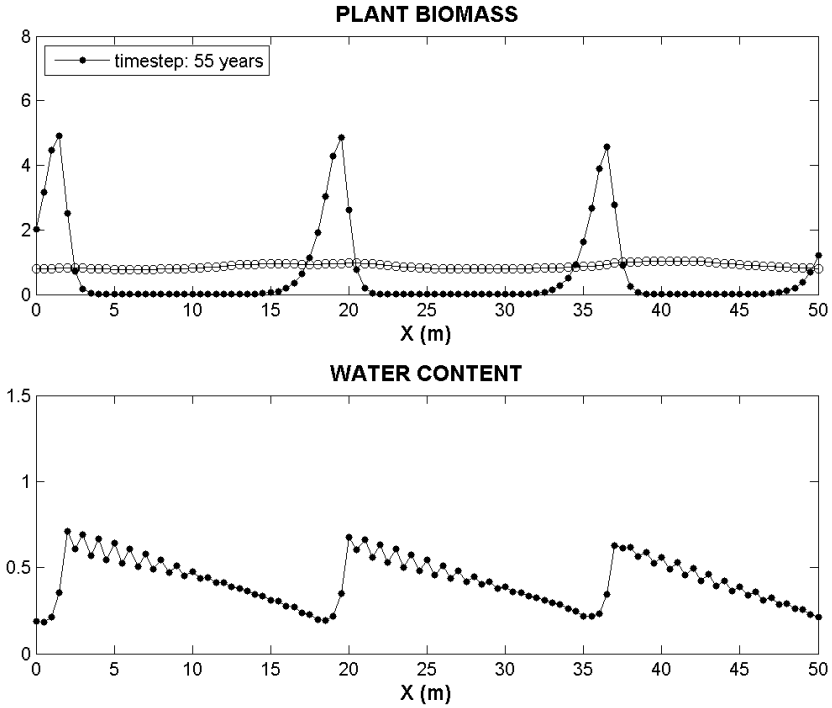

Figure 19: K99 with direct competition. Patterns configuration after a 55 years simulation time.

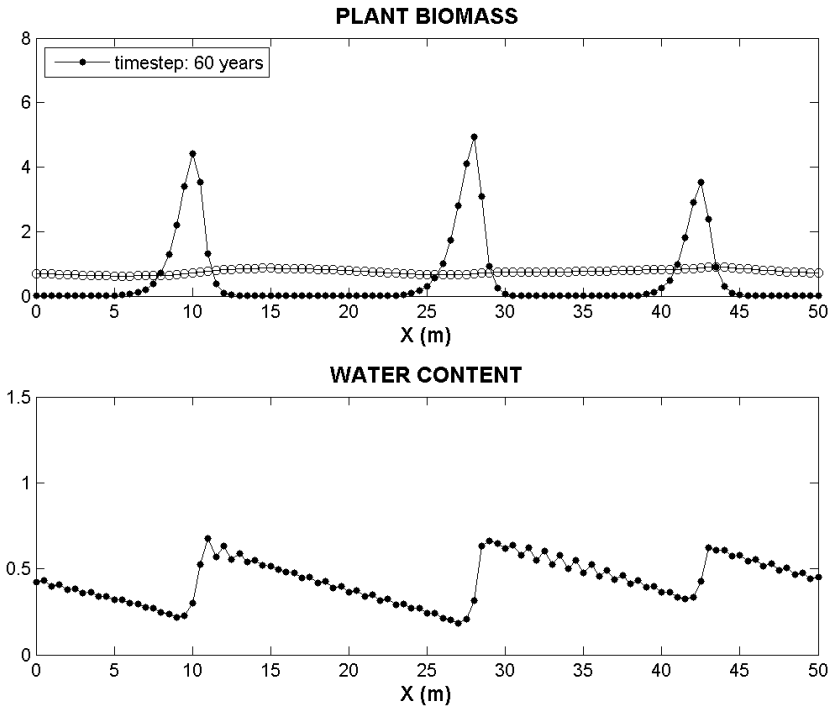

Figure 20: K99 with direct competition. Patterns configuration after a 60 years simulation time.

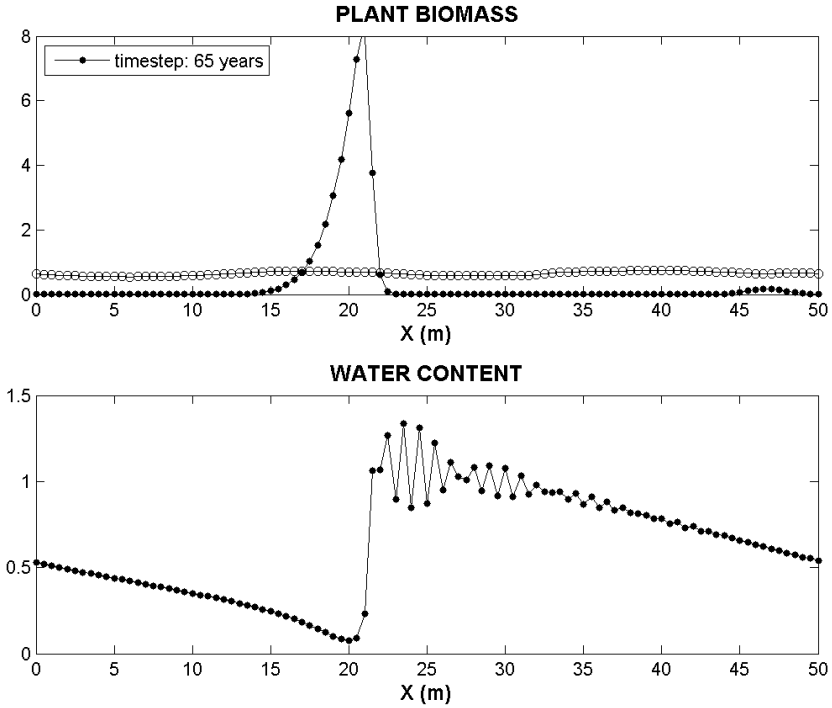

Figure 21: K99 with direct competition. Patterns configuration after a 65 years simulation time.

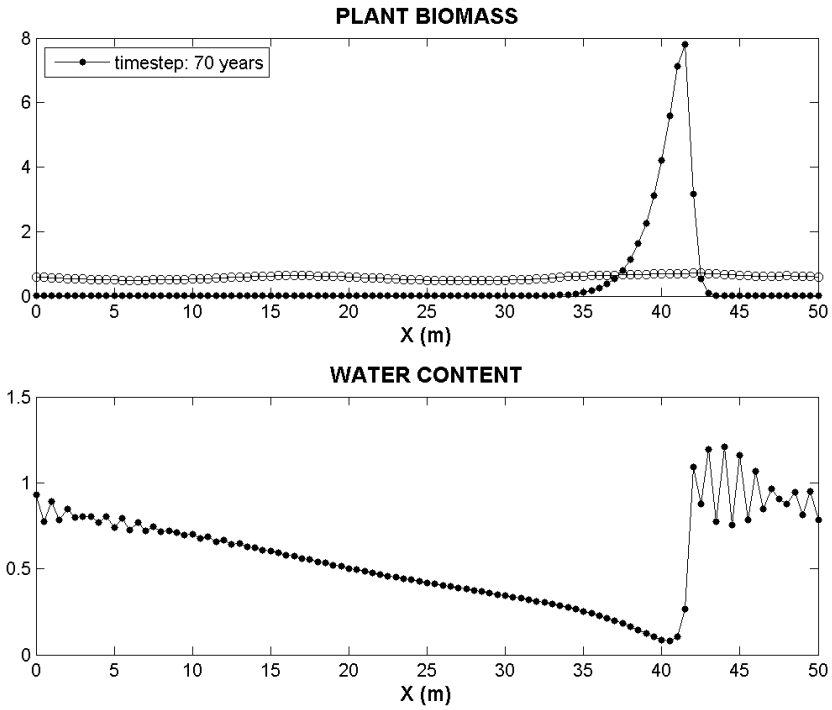

Figure 22: K99 with direct competition. Patterns configuration after a 70 years simulation time.

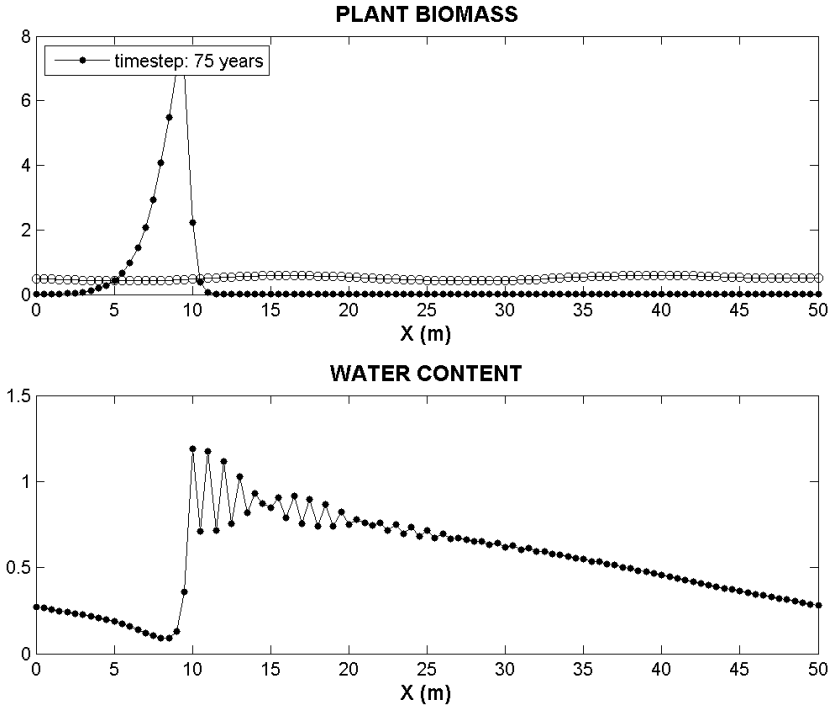

Figure 23: K99 with direct competition. Patterns configuration after a 75 years simulation time.

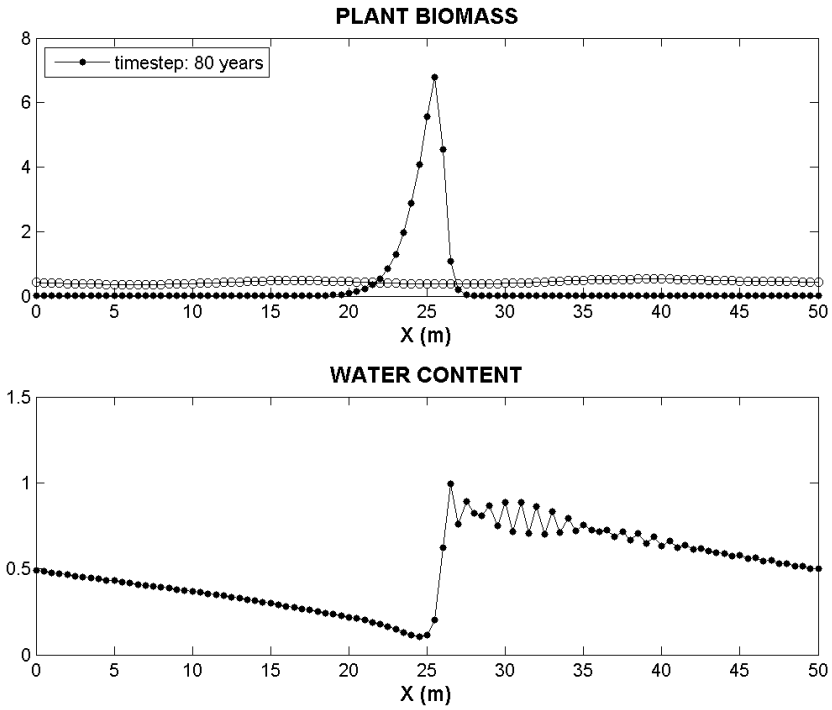

Figure 24: K99 with direct competition. Patterns configuration after a 80 years simulation time.

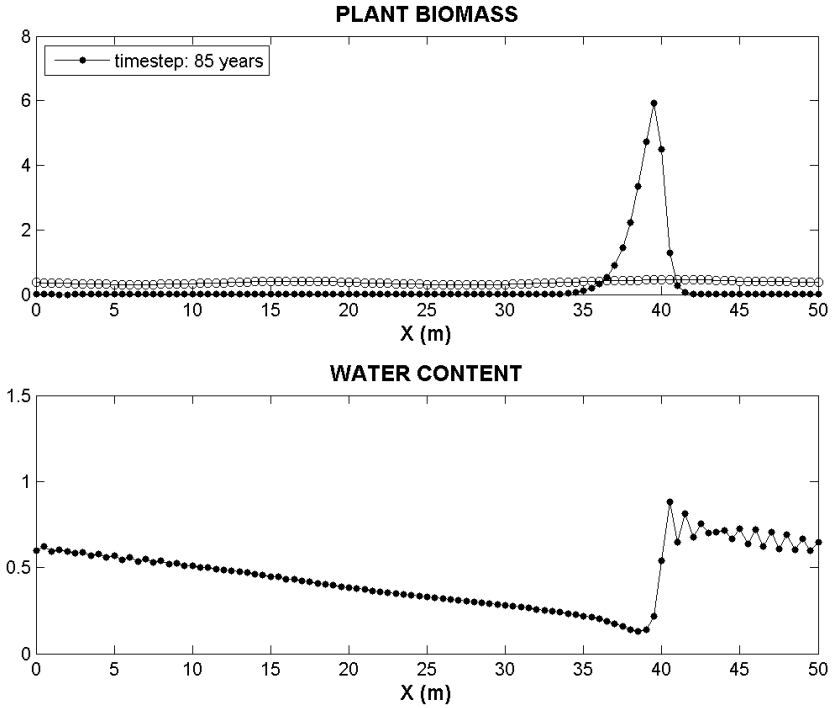

Figure 25: K99 with direct competition. Patterns configuration after a 85 years simulation time.

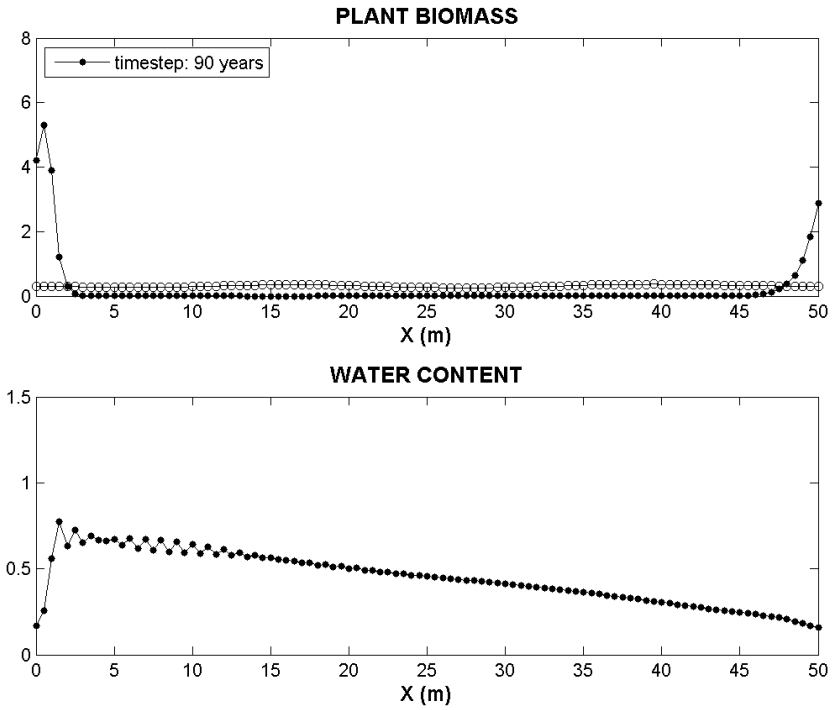

Figure 26: K99 with direct competition. Patterns configuration after a 90 years simulation time.

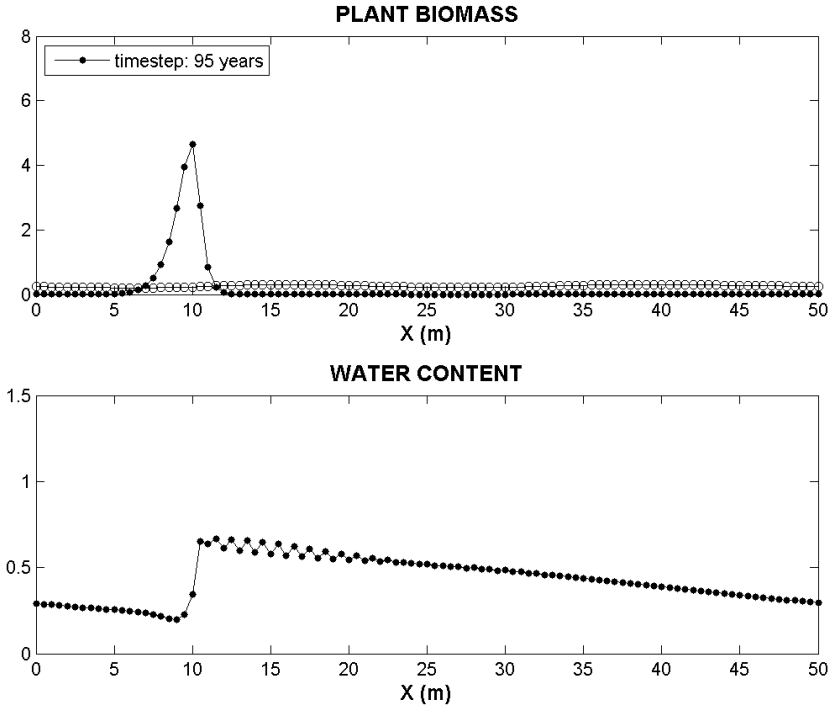

Figure 27: K99 with direct competition. Patterns configuration after a 95 years simulation time.

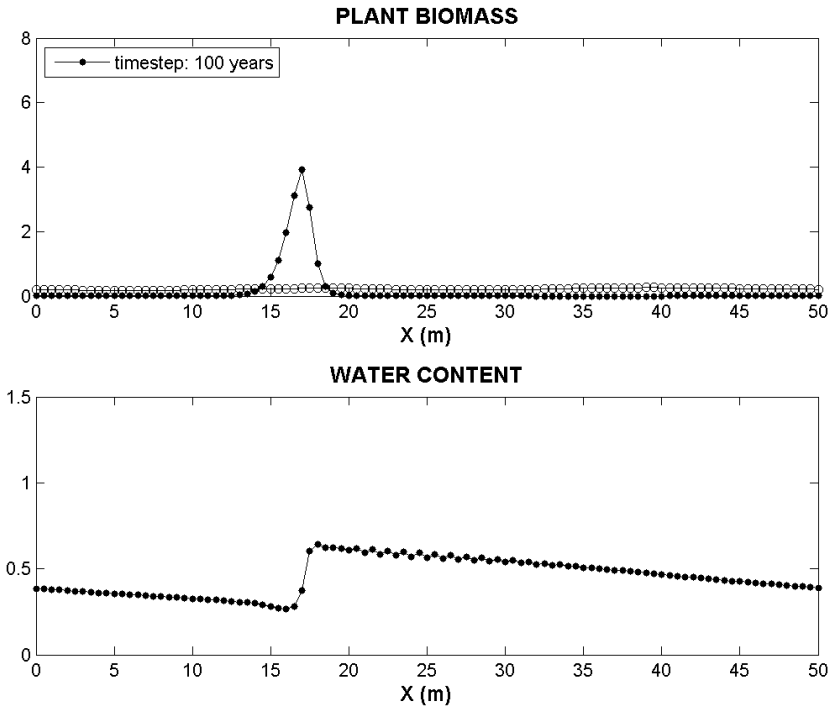

Figure 28: K99 with direct competition. Patterns configuration after a 100 years simulation time.

Adding a small perturbation to the homogeneous steady state solutions leads to instability because of the spatial effects. Patterns always emerge within five years, and they stay quite regular for at least 25 years, but they never reach a steady spatial configuration, in fact they degenerate after a 25-30 years period. This happens for all the models we implemented that consider a second competitive plants species that give patterns.

6 Conclusions

In this work, we focused on different species zonation in vegetation patterns. This aspect is a major feature in tiger bush landscapes, but it still had not been formally considered within the frame of mathematical modelling.

We first developed an analytical procedure that allowed us to study the linear stability of the different models, in their homogeneous and non-homogeneous form, in order to determine whether the model would give patterning, and to identify appropriate set of parameters.

The models we considered were built by adding a third equation to the original model of Klausmeier, and conveniently modifying the first two equations, in order to consider inter-species facilitation-competition dynamics.

Finally, we analyzed the models outputs, finding that two models in particular, one based on Klausmeier's growth function and one based on Tilman's growth function, predict a spatial zonation of the band, with one species acting as a pioneer and colonizing new sites in uphill positions, and the other species occupying the core of the band and exploiting most of the water availability. However, the patterns emerging from these models never reach a steady spatial configuration, on the contrary, they tend to degenerate after a 25-30 years period.

These results open more questions on what the actual role of each species is within the band. Competition for resources partially explains the band zonation, but some facilitation effects may exist that have been ignored until now although they may be responsible of patterns stabilization in time. Further investigations are needed to comprehend how the infiltration rate is affected by different plant species. Moreover, we retained the Klausmeier's

hypothesis of a constant water supply, but the actual rainfall supply in arid and semi-arid lands is only concentrated in two short wet seasons, so this may suggest that taking into account a more realistic rainfall distribution and different responses of the two plant species to water shortage during dry seasons could play an important role in stabilizing the modelled patterns.

In conclusions, this work partially answers to the initial question, showing that the inter-species competition for resources is responsible of zonation within bands. Nevertheless, it also leads to new questions that suggest further investigations and hopefully future developments in the vegetation patterns studies.

References

Boaler, S., & Hodges, C. (1964). Observations on vegetation arcs in the northern region, Somali Republic. *Journal of Ecology, 52*, pp. 511-544.

Borgogno, F., D'Odorico, P., Laio, F., & Ridolfi, L. (2009). Mathematical models of vegetation pattern formation in ecohydrology. *Rev. Geophys., 47*.

Clos-Arceduc, A. (1956). Etude sur photographies aériennes d'une formation végétale sahélienne: La brousse tigrée. *Bull. Insts. Fondam. Afr. Noire, Ser. A, 18(3)*, pp. 677-684.

Deblauwe, V., Couteron, P., Bogaert, J., & Barbier, N. (2012). Determinants and dynamics of banded vegetation pattern migration in arid climates. *Ecological Monographs, 82*, pp. 3-21.

Galle, S., Ehrmann, M., & Peugeot, C. (1999). Water balance in a banded vegetation pattern A case study of tiger bush in western Niger. *Catena, 37*, pp. 197–216.

Goutorbe, J.-P., Lebel, T., Tinga, A., Bessemoulin, P., Brouwer, J., Dolman, A., . . . Wallace, J. (1994). HAPEX-Sahel: a large scale study of land-atmosphere interactions in the semi-arid tropics. *Annales Geophysicae, 12*, pp. 53-64.

Greig-Smith, P. (1979). Pattern in vegetation. *Journal of Ecology, 67*, pp. 755-779.

HilleRisLambers, R., Rietkerk, M., van den Bosch, F., Prins, H., & de Kroon, H. (2001). Vegetation pattern formation in semi-arid grazing systems. *Ecology, 82(1*, pp. 50-61.

Klausmeier, C. A. (1999). Regular and irregular patterns in semiarid vegetation. *Science, 284(5421)*, pp. 1826–1828.

Lefever, R., & Lejeune, O. (1997). On the origin of tiger bush. *Bull. Math. Biol., 59(2)*, pp. 263–294.

Leprun, J. (1999). The influences of ecological factors on tiger bush and dotted bush patterns along gradients from Mali to northern Burkina Faso. *Catena, 37*, pp. 25-44.

Macfadyen, W. (1950). Soil and vegetation in British Somaliland. *Nature, 4186*, p. 121.

Macfadyen, W. (1950). Vegetation patterns in the semi-desert plains of British Somaliland. *The Geographical Journal, 116*, pp. 199-211.

Menaut, J.-C., Saint, G., & Valentin, C. (1993). SALT, les Savanes à Long Terme. Analyse de la dynamique des savanes de l'afrique de l'Ouest: méchanismes sou-jacent et spatialisation des processus. *Lettre du Programme Environnement, CNRS, 10*, (pp. 34-36).

Michaelis, L., & Menten, L. (1913). Die Kinetik der Invertinwirkung. *Biochem. Z., 49*, pp. 333–369.

Murray, J. D. (2002). *Mathematical Biology.* Berlin: Springer.

Rovinsky, A. B., & Menzinger, M. (1992). Chemical-instability induced by a differential flow. *Phys. Rev. Lett., 69(8)*, pp. 1193-1196.

Saco, P., & Moreno-de las Heras, M. (2013). Ecogeomorphic coevolution of semiarid hillslopes: Emergence of banded and striped vegetation patterns throught interaction of biotic and abiotic processes. *Water Resource Research, 49*, pp. 115-126.

Seghieri, J., Galle, S., Rajot, J., & Erhmann, M. (1997). Relationships between soil moisture and growth of herbaceous plants in a natural vegetation mosaic in Niger. *Journal of Arid Environments, 36*, pp. 87-102.

Sherratt, J. (2005). An analysis of vegetation stripe formation in semi-arid landscapes. *Mathematical Biology, 51*(183–197).

Thiery, J. M., D'Herbes, J.-M., & Valentin, C. (1995). A model simulating the genesis of banded vegetation patterns in Niger. *J. Ecol., 83(3)*, pp. 497–507.

Tilman, D. (1994). Competition and Biodiversity in Spatially Structured Habitats. *Ecology, 75*, pp. 2-16.

Turing, A. M. (1952). The chemical basis of morphogenesis. *Philos. Trans. R. Soc., Ser. B, 237,*, pp. 37-72.

Ursino, N. (2005). The influence of soil properties on the formation of unstable vegetation patterns on hillsides of semiarid catchments. *Adv. Water Res., 28(9)*, pp. 956–963.

Ursino, N. (2007). Modeling banded vegetation patterns in semiarid regions: Interdependence between biomass growth rate and relevant hydrological processes. *Water Resour. Res., 43*.

Valentin, C., & D'Herbès, J. (1999). Niger tiger bush as a natural water harvesting system. *Catena, 37*, pp. 231–256.

Valentin, C., D'Herbès, J. M., & Poesen, J. (1999). Soil and water components of banded vegetation patterns. *Catena, 37(1–2)*, pp. 1-24.

Wallace J. S., & Hollwill, C. (1997). Soil evaporation from tiger bush in south-west Niger. *Journal of Hydrology, 188-189*, pp. 426-442.